DOKUZ EYLÜL UNIVERSITY

GRADUATE SCHOOL OF NATURAL AND APPLIED SCIENCES

DEVELOPMENT OF A NOVEL SPHERICAL LIGHT-BASED POSITIONING SENSOR IN SOLAR TRACKING

by

Oğuz GORA

March, 2022

İZMİR

DEVELOPMENT OF A NOVEL SPHERICAL LIGHT-BASED POSITIONING SENSOR IN SOLAR TRACKING

A Thesis Submitted to the

Graduate School of Natural and Applied Sciences of Dokuz Eylül University

In Partial Fulfillment of Requirements for the Degree of Doctor of Philosophy in Mechatronics Engineering

by

Oğuz GORA

March, 2022

İZMİR

Ph.D. THESIS EXAMINATION RESULT FORM

We have read the thesis entitled **"DEVELOPMENT OF A NOVEL SPHERICAL LIGHT-BASED POSITIONING SENSOR IN SOLAR TRACKING"** completed by **Oğuz GORA** under supervision of **Assistant Prof. Dr. Taner AKKAN** and we certify that in our opinion it is fully adequate, in scope and in quality, as a thesis for the degree of Doctor of Philosophy.

Assistant Prof. Dr. Taner AKKAN

Supervisor

------------------------------	-------------------------------------
Prof. Dr. Zeki KIRAL	Prof. Dr. Engin KARATEPE
Thesis Committee Member	Thesis Committee Member

------------------------------	-------------------------------------
Prof. Dr. Mustafa GÜNDÜZALP	Prof. Dr. Mutlu BOZTEPE
Examining Committee Member	Examining Committee Member

Prof. Dr. Okan FISTIKOĞLU

Director

Graduate School of Natural and Applied Sciences

ACKNOWLEDGEMENTS

I would firstly like to thank to my supervisor Asst. Prof. Dr. Taner AKKAN who provided full support during all phases of this thesis. It wouldn't be possible to complete this study without his valuable guidance and contributions.

I also want to thank committee members of my doctorate thesis Prof. Dr. Zeki KIRAL and Prof. Dr. Engin KARATEPE. Their contributions and criticisms during the formation of the thesis greatly contributed to my study and my academic development.

Also, I want to thank Prof. Dr. Mustafa GÜNDÜZALP and Prof. Dr. Mutlu BOZTEPE who took part in my doctorate thesis defense for their contributions during my defense.

I would also like to thank Dokuz Eylül University for providing worldwide patenting (PCT) support for the design, which is one of the outputs of this thesis.

I am deeply grateful to my father Ahmet GORA, whom I lost in a recent time, for motivating and giving technical countenance to me, and to my mother Nurhayat ÖZEL for her emotional support.

Lastly I would like to thank my friend İsmet ATEŞ, for his suggestions and contributions to my thesis process.

Oğuz GORA

DEVELOPMENT OF A NOVEL SPHERICAL LIGHT-BASED POSITIONING SENSOR IN SOLAR TRACKING

ABSTRACT

The demand for solar energy among alternative energy sources has been increasing in recent years. Despite the increasing demand for solar energy and the great potential in solar energy, the efficiency of energy systems using solar energy still has not reached the desired levels. One of the methods to increase the energy produced from these systems is solar tracking systems.

Many academic studies have been conducted on solar tracking systems. On the other hand, the need for a cost-effective, easily accessible, high-accuracy sensor that does not require much processing power continues for effective tracking of the sun.

In this study, a unique sensor was designed to localize the sun in the sky to be used in solar tracking systems. The solid model of this sensor is designed and manufactured spherically. Thanks to the spherical form of the sensor, the need for a transformation of the measured data is eliminated. This produced sensor collects data with the help of a measurement system and transfers these data to the computer environment. Necessary studies (checksum control, speed tests, etc.) have been carried out to transfer these data at an appropriate speed and without errors. In addition, the measurement data were taken with using the Time Synchronous Averaging (TSA) method and cleared of noise and high frequency components. In the last part of the study, the localization of the light source in azimuth and elevation angles is provided with the help of the algorithm that uses a fuzzy logic model. In addition, visual outputs related to the localization of the light source were obtained by visualizing the measurement data in spherical form.

Keywords: Solar tracking systems, sun sensor, measurement systems, time synchronous averaging method, fuzzy logic applications.

GÜNEŞ TAKİBİNDE ÖZGÜN BİR IŞIK-BAZLI KONUMLANDIRMA SENSÖRÜNÜN GELİŞTİRİLMESİ

ÖZ

Alternatif enerji kaynakları arasında güneş enerjisine talep son yıllarda giderek artmaktadır. Güneş enerjisine talebin giderek artması ve güneş enerjisinde büyük potansiyele rağmen güneş enerjisi kullanılan enerji sistemlerinin verimliliği halen istenilen düzeylere erişememiştir. Bu sistemlerden elde edilen enerjiyi arttıracak yöntemlerden biri güneş takip sistemleridir.

Güneş takip sistemlerine ilişkin birçok akademik çalışma yapılmıştır. Buna karşın güneşin etkin bir şekilde takibi için uygun maliyetli, kolay erişilebilir, doğruluğu yüksek, fazla işlemci gücü gerektirmeyen sensör ihtiyacı devam etmektedir.

Bu çalışmada, güneş takip sistemlerinde kullanılmak üzere güneşin gökyüzünde lokalizasyonunun sağlanması için özgün bir sensör tasarlanmıştır. Bu sensörün katı modeli küresel olarak tasarlanmış ve üretilmiştir. Sensörün küresel formu sayesinde ölçülen verilerde bir dönüşüm ihtiyacı ortadan kalkmıştır. Üretilen bu sensör bir ölçüm sistemi yardımıyla verileri toplamakta ve bu verileri bilgisayar ortamına taşımaktadır. Bu verilerin uygun hızda ve hatasız taşınması için gerekli çalışmalar (checksum kontrolü, hız testleri vb.) yapılmıştır. Ayrıca ölçüm verileri Zaman Senkronizasyonlu Ortalama (ZSO) metodu ile alınarak gürültüler ve yüksek frekans bileşenlerinden temizlenmiştir. Çalışmanın son kısmında bulanık mantık modelinin de kullanıldığı algoritma yardımıyla ışık kaynağının azimuth ve elevation açılarında lokalizasyonunu sağlanmaktadır. Bunun yanında ölçüm verileri küresel formda görselleştirilerek ışık kaynağının lokalizasyonuna ilişkin görsel çıktılar da elde edilmiştir.

Anahtar kelimeler: Güneş takip sistemleri, güneş sensörü, ölçüm sistemleri, zaman uyumlu ortalama metodu, bulanık mantık uygulamaları.

CONTENTS

LIST OF FIGURES

Page

LIST OF TABLES

CHAPTER ONE

INTRODUCTION

1.1 Motivation of Thesis

Energy production has been of great importance since the beginning of the industrial revolution. It is not possible for us to use all the tools that enable to maintain our modern life without an energy source. However, energy production has been one of the priority problems of countries. The nature of the problem arises from the fact that energy resources are limited, their costs are high, their access is difficult, and they can be environmentally harmful. When fossil energy resources are considered, the fact that only certain countries own these resources makes it difficult and costly for other countries to access these resources. In addition, there is a production decrease and depletion of these resources in the foreseeable future. It is now a scientifically accepted reality that fossil fuels cause serious environmental problems – especially the global climate crisis.

Alternative energy sources are energy sources that have the potential to solve the aforementioned problems to a certain extent (Owusu & Asumadu-Sarkodie, 2016; Sims, 2004) Energy production with these resources is not only based on fossil resources owned by certain countries, but allows many countries to produce energy in a more environmentally friendly way with more affordable costs. In addition, energy production with these resources can be done centrally as well as in decentralized and local areas. This is also a supporting feature of the local energy production and consumption paradigm, which is widely adopted today.

Among these sources, solar energy is in a different position from other energy sources in terms of its environmentalist feature and high energy potential. In some geographical locations where the energy transmitted by the solar radiation reaching the earth is high (especially the countries located near the Equator and that belt), 1400 Watts per square meter is reached. (Darula, Kittler, & Gueymard, 2005; Drummond, Hickey, Scholes, & Laue, 1968). In terms of the efficiency of the installed systems, this point indicates a great potential.

Despite the high potential in question, the systems established for the generation of electrical energy from solar energy still have not reached the desired efficiency levels. At this point, the amount of energy that enters the cycle, namely solar energy, is as important as the conversion technology in which solar energy is converted into electrical energy.

When the use of solar energy, both photovoltaic, thermal and all of the systems in which these are combined, are evaluated, increasing the amount of energy entering the system will significantly increase the amount of electrical energy produced from the facility. In order to do this by keeping the surface area constant, keeping the solar energy concentrated is one of the preferred methods. The other works on receiving surfaces that optimally capture - track - the solar beam with varying incidence angles. The main motivation of this thesis is to design a unique spherical solar sensor that produces high-accuracy outputs for solar tracking systems to localize the sun. For this purpose, a solid model of the sensor structure was produced. It works together with light sensors and electronic circuits placed on this structure. Fuzzy logic is applied for the localization of the sun as the light source.

1.2 Literature and Research Gap

In recent years, the dynamism and projections in the world's energy markets reveal a future potential in which serious changes can occur in energy production and consumption. A world where energy efficiency increases, low-carbon economy comes to the fore, and the increase in energy demand is tried to be reduced is a topic of discussion -discussed by- for the political and academic environments (Birol, 2006; Smith, 2012)

As part of these discussions, the popularity of solar energy has increased among countries aiming to transition to renewable energies. Studies are carried out both in the conversion technologies of solar energy to electrical energy and in the point of making the most efficient use of solar energy with existing technologies. For example, in addition to poly-crystalline photovoltaic technologies, significant progress have been made in the conversion from solar energy to electrical energy with solar cells produced with organic or inorganic materials or dye sensitized (DSSC). (Dezfooli, Nejad, Zakeri, & Kazemifard, 2017; Qiu, Ono, & Qi, 2018; Roslan et al., 2018). Similar advances have been made in systems that focus the solar beam on specific points by creating concentrated solar energy systems. The systems operating at high temperatures can still provide high energy conversion efficiencies (Barlev, Vidu, & Stroeve, 2011).

Solar tracking systems is a subject that has been studied for the last 20 years in order to use the existing technologies in the most efficient way. There have been many studies in the literature that differ from each other in terms of degrees of freedom, tracking strategy, control method, and driving method. These studies are discussed in detail in Section 2.5.

Optimum positioning of the receiver surface is very important in solar tracking systems since the efficiency of the system depends on it. In order to do this, it is necessary to determine the location of the sun in the sky correctly or to direct the receiving surfaces to the positions that will provide the highest efficiency indirectly.

Sidek et al., (2014) obtains latitude and longitude information by using the Global Positioning System (GPS) in their study. They calculate the current position of the sun in the sky by using astronomical equations and time information. With the help of magnetic sensors, they calculate the geographical north direction according to the magnetic field of the earth and directs the photovoltaic panels to the desired positions in azimuth and altitude angles.

Samanta, Dutta, & Neogi, (2012) used Light Dependent Resistor (LDR) as a frequently preferred method in their studies. The position of the sun in the sky is tried to be determined with the help of LDRs placed in the East-West and North-South directions. The installed system is controlled with the help of Programmable Logic Controller (PLC). The study emphasizes both that dual-axis tracking systems are more efficient than single-axis tracking systems and the importance of the flexibility provided by PLC control.

Tina, Arcidiacono, & Gagliano, (2013) detect the position of the sun in the sky with 9 photodiodes placed on the plastic surface in their work. Sun shade and light are used as critical parameters in the study. When the sun is not perpendicular to the surface, it creates a shadow and this gives information about the angular position of the sun in the sky.

Garrido & Díaz, (2016) created a system that detects the elevation angle of the sun with the photodiodes placed in the cylinder they specially designed for their work. A closed loop was created with a Proportional and Integral (PI) controller. The voltage difference measured over the photodiodes is used as the working principle. The maximum tracking error in the system is calculated with the Mean Square Error (MSE) and is obtained as 0.134˚.

Wei, Xing, Li, & You, (2011) worked on the design of a digital sun sensor. The system created by using a charge-coupled detector (CCD) can measure the position of the sun in the East-West and North-South directions. An N-shaped slit, Micro-electromechanical System (MEMS) and CCD device are used. It is stated that the system has the advantages of in terms of size, weight and low energy consumption.

Pita et al., (2014) designed a pyramidal sensor for satellites in their work. 5 light cells placed in the shape of a pyramid are used in the electronic circuit with a simple mathematical algorithm. The design has a unique physical structure among sun sensors.

Lee et al., (2015) designed a hybrid sun sensor in their study. A square prism, 4 photodiodes and a hemispherical cap are used. The principle is to cast a shadow on one or two photodiodes under the influence of the sun and take advantage of the differences in electrical currents. In addition, astronomical calculations are made by using the data obtained with the help of GPS in cases where the sun's rays are lower than 400 W/m^2. Thus, a system that can operate in low radiation conditions has been established.

Abdollahpour, Golzarian, Rohani, & Abootorabi Zarchi, (2018) ‘s work has been an original solar tracking system. A rod is placed perpendicular to the top of the receiving surface and the surface on which its shadow is projected was observed with the camera. The zenith angle and height are determined by using the length of the shadow. A highly accurate solar tracking system is obtained by using linear regression and morphological methods.

When the studies on sun sensors and sun tracking systems in the literature are examined, the following results are found out:

- Although solar tracking systems installed with LDRs are useful in practice, they cannot produce highly accurate information about the sun's position in the sky.
- In systems that make use of astronomical calculations, GPS sourced location, time and date information is needed.
- Sensors using microelectronic or MEMS technology have disadvantages such as manufacturing difficulty and high cost.
- High computational capability is required in systems that calculate the position of the sun with image processing method or data obtained with intelligent control algorithms.
- The fact that some of the developed sensors are too sensitive to other parameters such as temperature, humidity, wind, cloudiness creates a disadvantage regarding the stable operation of the sensors.

The results obtained above show that there are still some research gaps in this research area and there are parts that can be contributed. These parts can be listed as follows:

- Solar sensors must be cost-effective and accurate enough to meet the desired needs.
- In systems with sun sensors, there should be no need for intensive calculations. The need for intensive computation increases both cost and software complexity.

- The fact that the sun sensor is ready for use wherever it is placed, independent of the geographical location information, will provide an advantage in terms of practicality.
- Sensors created using original physical bodies are still in development. Original and effective designs to be made on this subject will find use in this field.
- The fact that the sensor can be applied to different light sources as well as to a light source such as the sun can provide modularity and gain widespread use.

Considering these research gaps listed, first of all, it is aimed to develop a solution for the position of the sun in the sky with a unique physical structure. This solution is requested to work without using LDR, without the need for geolocation information. With this solution, the position of the sun in the sky will be determined using fuzzy logic. In addition, the developed design solution should be usable for light sources of different wavelengths, thanks to the modularity of the sensor structure.

1.3 Organization of Thesis

In the second chapter of the thesis, alternative energy sources and the importance of solar energy among these sources are discussed. In the same chapter, the sun geometry and sun angles that form depending on the sun are explained. Solar irradiation and solar tracking systems are also discussed in this chapter.

In the third chapter of the thesis, the model in which the light sources are sensed spherically is explained. In this context, the solid model, electronic systems and general characteristics of the sensor are discussed.

In the fourth chapter, data collection methods with the developed sensor are evaluated. Samples are collected with manual and automatic measurement techniques. In the fifth chapter of the study, the fuzzy logic structure used and its application on the developed sensor are discussed. In this context, the general structure of the fuzzy logic system used is explained. In the sixth chapter, the conclusions drawn and their evaluation are made and future studies and predictions in this field are shared.

CHAPTER TWO

ALTERNATIVE ENERGY SOURCES AND SOLAR ENERGY

2.1 Alternative Energy Sources

Energy sources known as conventional energy sources are energy sources based on fossil fuels. These resources can be listed as petroleum, coal and natural gas and their derivatives. These energy sources, which have been used from the beginning of the industrial revolution to the present, have various effects on societies. The first of these effects is the economic effect. Figure 2.1 shows the change in oil barrel price over the years.

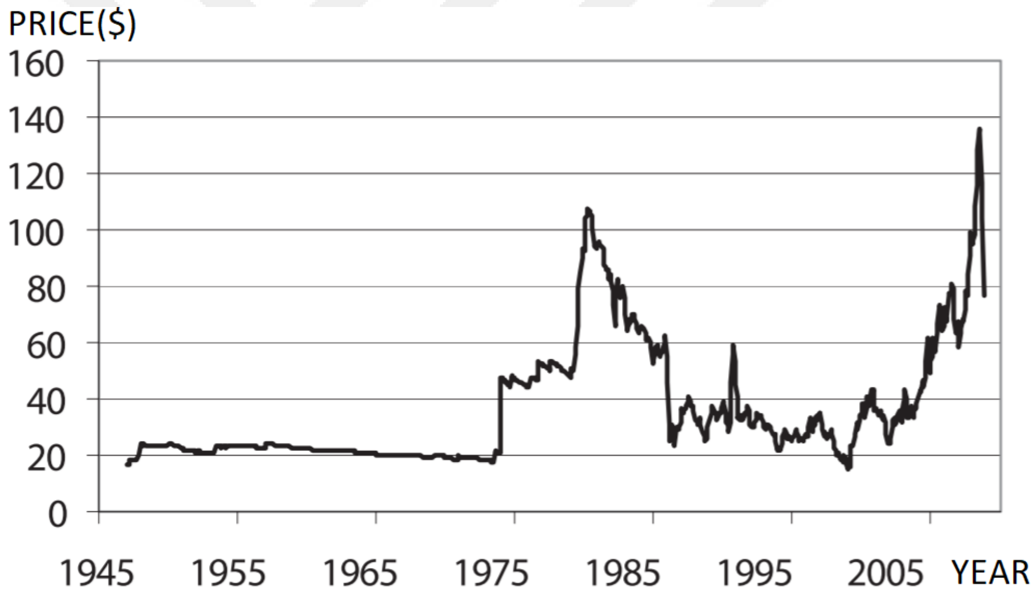

Figure 2.1. Oil Prices by Years (Hamilton, 2009).

As can be seen, there are extreme fluctuations and changes in oil prices during periods of social crises or economic recessions (especially the years 1974, 2001, 2008, 2018). This situation does not create an economically sustainable environment. However, since the countries where oil and petroleum-derived energy resources are found and extracted are limited to certain countries around the world, the access of other countries to these energies creates problems both economically and strategically.

Another issue that should be listed in terms of the effects of these energy sources is their environmental effects. These fossil energy sources cause the emission of gases that will create a greenhouse effect in the atmosphere, whether they are used in power plants or used in automobiles or for heating purposes. These gases are mainly carbon dioxide (CO_2), methane (CH_4), nitrous oxide (N_2O), hydrofluorocarbon gases. In addition to the emission of greenhouse gases into the atmosphere, the use of these sources as an energy source leads to the emergence of an economy based on the circulation of carbon in both industry and residences. This causes an effect that supports global warming, which spreads to the whole of social and economic life. Moreover, it is necessary not to ignore the carcinogenic properties of raw materials such as plastic, asphalt and various petro-chemicals produced with petroleum-derived substances, polluting the nature, threatening the living life.

Considering all these listed effects, countries have turned to search for different energy sources in recent times. These sources, which are called alternative energy sources, are solar energy, wind energy, hydraulic energy, geothermal energy, biomass energy, wave energy and nuclear energy. In recent years, newly developed energy technologies, whose effects are still small, are also considered within the scope of alternative energy sources (Ak & Demirbas, 2016) (Skilhagen, 2010) (Suarez & Luengo, 2003).

Some of these alternative energy sources are renewable and allow energy production without the need for a source other than natural energy effects from outside, while a source such as nuclear energy does not have a renewable energy feature, although it needs constant fuel use. Again, in terms of environmental effects, it is difficult to say that alternative energy sources are completely environmentally friendly. Although nuclear energy, hydraulic energy, geothermal energy and biomass energies have different impact levels, they continue to carry a risk potential.

Among the alternative energy sources, especially solar energy has the potential to create serious beneficial changes in the energy market with its low environmental impact and high energy potential. For this reason, today alternative energy has been primarily preferred type of energy that many countries setting targets for aiming to transitioning to renewable energy.

2.2 Solar Energy

The sun is an energy source located approximately 149 million kilometers from our earth. The energy released as a result of thermonuclear reactions in the sun spreads to the earth and other planets.

The heat and light reaching to our world from the sun are the source of life on earth. Plants can perform photosynthesis thanks to sunlight. Different air pressures occur due to the different amounts of warming of the regions on the earth. This provides the emergence of air currents that will cause winds and climatic events. Fossil fuels (coal, oil, etc.) are also formed thanks to the chemical energy stored in living things due to the effects of solar beams.

Limited amount of the energy emitted from the sun reaches the earth. Approximately half of the 150,000 TW energy emitted reaches the earth's surface. Figure 2.2 represents the parts of the energy emitted from the sun that are reflected by the atmosphere and the earth's surface, and absorbed by the atmosphere and clouds.

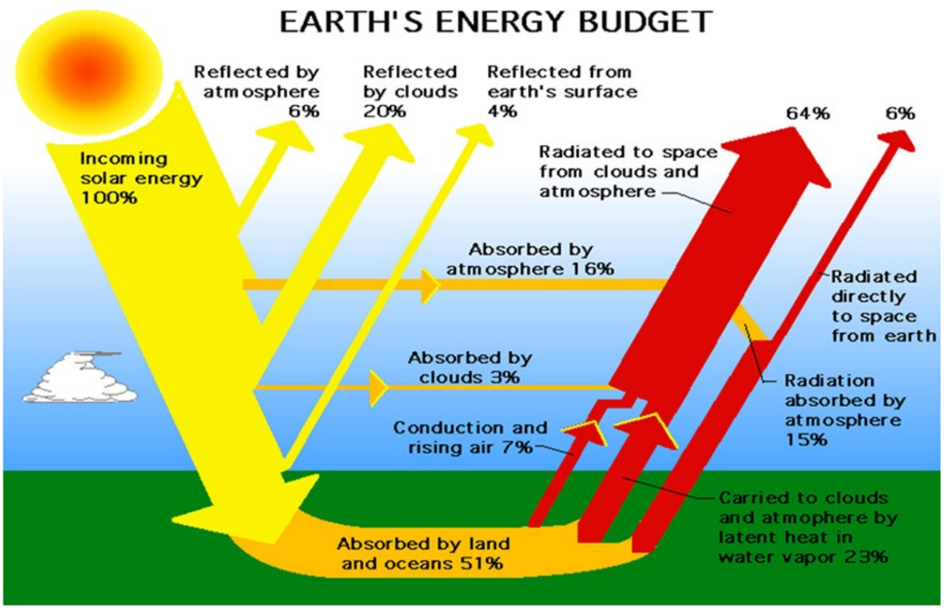

Figure 2.2 Energy Budget (NASA, n.d.).

The energy of the sun reaching the earth creates an electromagnetic spectrum covering various wavelengths. This spectrum includes the visible wavelengths of light to the naked eye and the ultraviolet wavelengths outside the visible region. Spectrum gives information about the amount of energy contained in the solar beams in Watts / m^2. Since various receiver surfaces are used in applications related to solar energy, the wavelength of the solar beams and the amount of energy they carry are important. The energy carried by photons emitted from the sun is expressed by the following formula:

$$E = hv = \frac{hc}{\lambda} \tag{2.1}$$

h: Plank Constant v: Frequency c: Speed of Light λ: Wavelength

The solar spectrum formed by the solar beams at different wavelengths is shown in Figure 2.3.

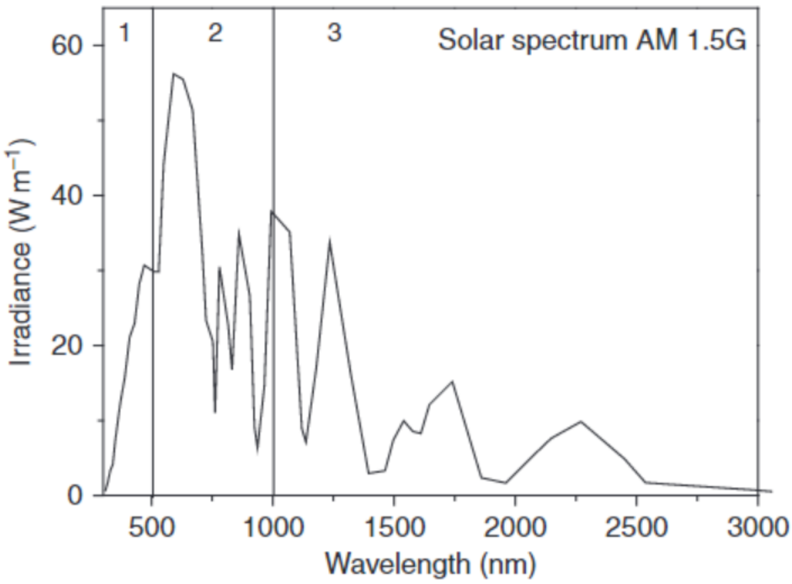

Figure 2.3. Solar Spectrum (Jestin, 2012).

The AM (Air Mass) value in Figure 2.3 is defined as AM = 1 / cos (Θ_z) (S. Kalogirou, 2009). The Θ_z angle is the zenith angle, which is the angle between the surface normal of a point on the earth and the position of the sun. AM 1.5 G is generally accepted as the standard spectrum, and its global expression refers to the sum of direct solar radiation and reflected solar radiation. In the spectrum, low wavelengths are expressed with 1 region, 500 – 1000 nm wavelength part with intense energy with 2 regions, infrared region of the spectrum with 3 regions (Jestin, 2012).

2.3 Solar Geometry

The amount of sun beams reaching the earth's surface depends on the geometric relationship of the earth and the sun. The rotation of the Earth around its axis and around the sun is a combination of 3 different movements: axial tilt, wobble, orbit (Sen, 2008).

The first of these is axial tilt, which refers to the angle between the earth's orbit and the equatorial plane. In the hemisphere where the inclination towards the sun occurs, summer is experienced and when it is further away, winter is experienced. The tilt due to the rotation of the sun changes cyclically from 21˚45' to 24˚15'. This change takes place over a period of 42 000 years. (Sen, 2008). Wobble is the slip that occurs as the earth rotates on its axis. Its effect is seen over long periods of time. (Eubanks, 1993).

While the Earth's orbit exhibits an elliptical motion to revolve around the sun in one year, it completes its rotation in one day. (Sen, 2008). Thus, the earth's orbit and the tilt of its axis provide the seasons. Figure 2.4 shows the seasons that occur according to the earth's axis.

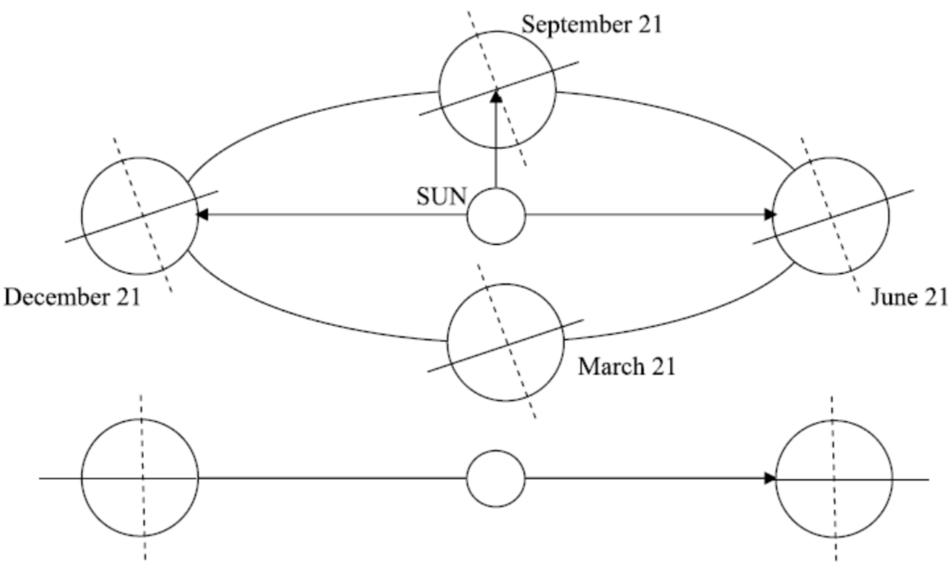

Figure 2.4 Seasons due to the tilt of earth’s axis (Sen, 2008).

2.3.1 Solar Angles

Some descriptive aspects arise due to the movements of the Earth and the Sun. The most important of these is the declination angle. The declination angle (δ) is an angle that results from the axial tilt of the earth as it rotates around the sun and around its axis. This angle is the angle between the sun and the equatorial plane.

The axial tilt of the earth is 23.45° . This axial tilt value changes between positive/negative values throughout the year. During the autumn and spring equinoxes, the declination angle changes to 0 and the sun is exactly on the equatorial plane (Messenger & Abtahi, 2017). The declination angle is shown in the Figure 2.5.

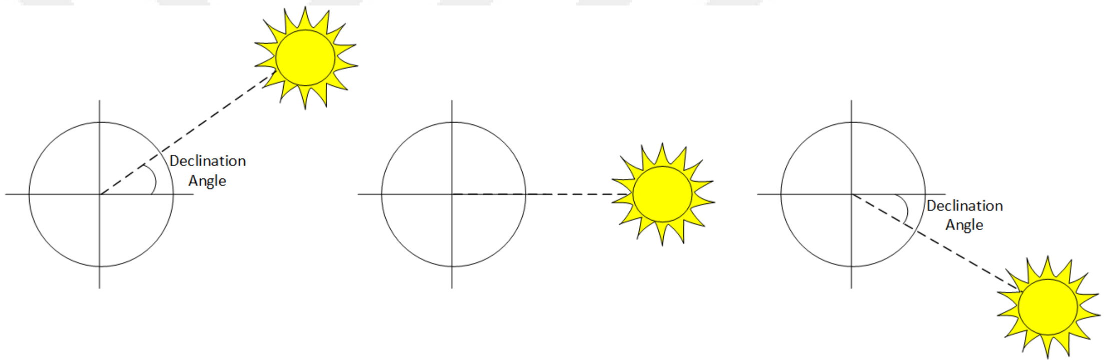

Figure 2.5 Declination Angle Relative to the Position of the Earth and Sun. Summer solstice in Northern hemisphere δ=23.45 ˚ (left). Spring equinox in northern hemisphere and autumn equinox in southern hemisphere δ=0 ˚ (center). Winter solstice in northern hemisphere and summer solstice in southern hemisphere δ=23.45 (right).

There are two expressions for calculating the declination angle. One of these two formulations results in radians and the other in degrees. These formulations are listed below (Messenger & Abtahi, 2017; Nsengiyumva, Chen, Hu, & Chen, 2018):

$$\delta = 23.45 \sin\left[2\pi \frac{n+284}{365}\right] \tag{2.2}$$

$$\delta = 23.45 \sin\left[\frac{360(n-81)}{365}\right] \tag{2.3}$$

n represents the day of the year.

On the other hand, the Zenith angle, is an angle that emerges from the geometric relationship between the Sun and the Earth. Zenith angle is defined as the angle between the sun and the surface normal of the geographical location found. (Jestin, 2012). The zenith angle is shown in Figure 2.6.

Another term, the solar hour angle, is the temporal expression of the sun relative to the noon hour. (S. C. Bhatia, 2014). Indicates the amount of deviation from the Sun's geographic south direction. It is formulated as follows (Nsengiyumva et al., 2018):

$$\omega = \frac{Minutes\ before\ noon(\text{min})}{4} \tag{2.4}$$

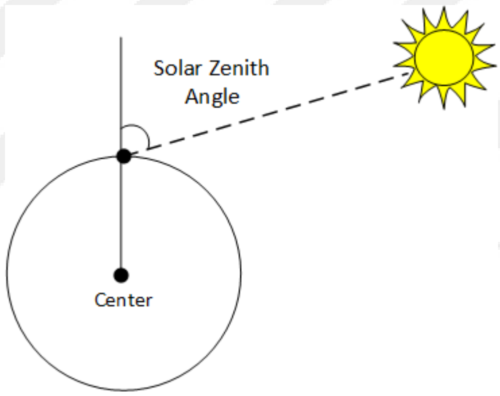

Figure 2.6. Solar Zenith Angle.

2.3.2 Derived Angles and Calculations Based on Solar Angles

More specific information about the sun's position in the sky is also needed in solar energy applications or astronomical calculations. In order to determine the exact position of the sun, 3 coordinates are needed. One of them is the distance of the sun, the other two are the angles related to its position. In general, if the distance from the sun is considered constant, the position of the sun can be determined from two angles.

The first of these angles is the angle expressed as solar altitude or solar elevation *(α_s)*. It is the angle between the observer point on the earth and the sun in the horizontal plane. It can also be understood as the complement angle of the Zenith angle. Therefore, it can be expressed as:

$$\alpha_s = \frac{\pi}{2} - \Theta_z \tag{2.5}$$

The solar elevation angle can also be expressed as:

$$\alpha_s = \sin^{-1}[(\cos\varphi\cos\delta\cos\omega) + (\sin\varphi\sin\delta)] \tag{2.6}$$

φ represents latitude.

The other angle, the azimuth angle, refers to the angle that the projection of the sun's position makes with the magnetic north direction. It is calculated as follows (Nsengiyumva et al., 2018):

$$\gamma_s = \cos^{-1}\left[\frac{(\sin\alpha_s\sin\varphi) - \sin\delta}{\cos\alpha_s\cos\varphi}\right] \tag{2.7}$$

Solar azimuth and elevation angles are shown in Figure 2.7.

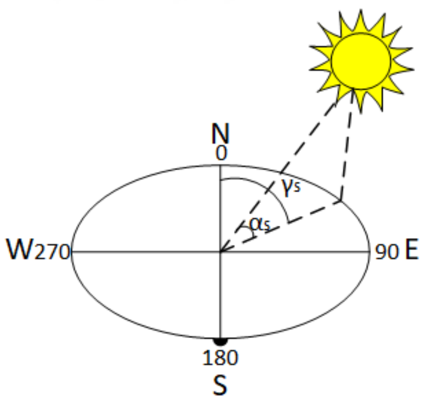

Figure 2.7 Solar Azimuth and Elevation Angles.

2.4 Clear Sky Solar Irradiation

The solar spectrum formed by the solar beam at different wavelengths, when it reaches the earth, instantly carries an energy value called the solar constant per unit area. (Darula et al., 2005). This amount of energy is expressed as:

$$I_{ON} = 1353\left[1 + 0.033\cos\frac{360n}{365}\right] \quad (2.8)$$

When the zenith angle (Θ_z) and the direct radiation transmittance of the atmosphere (τ_b) are taken into account, the carried energy is expressed as:

$$I_{cbhz} = I_{ON}.\cos(\Theta_z).\ \tau_b \quad (2.9)$$

In addition, the solar beam entering the atmosphere are also scattered through diffuse. This scattering can be determined according to the diffuse radiation τ_d transmittance, which varies depending on parameters such as climate type and altitude (Hottel, 1976). Diffuse radiation can be expressed as follows:

$$I_{cdhz} = I_{ON}.\cos(\Theta_z).\ \tau_d \quad (2.10)$$

The total amount of radiation reaching a point on the earth, on the other hand, can be expressed by using the amount of direct radiation and the amount of diffuse radiation together, as follows:

$$I_{cthz} = I_{cbhz} + I_{cdhz} \quad (2.11)$$

Considering all the solar angles and radiation equations in question, as an example calculation, 9 September 2018 for İzmir Bornova Evka-3 District (38°28'12.6" N, 27°14'52.7" E) at 14:00. Let's see the amount of radiation in:

Firstly,
I_{on} =1353[1+0.033 $cos(360n/365)$] = 1353 [1+ 0.033 cos(360∗252)/365] where n=252. There is the direct solar radiation I_{on}= 1369,329 W/m^2 .
The zenith angle (Θ_z) must be found in order to take into account the angle of incidence of solar radiation. Therefore, using the equations (2.5), (2.6), (2.2), (2.4) and by obtaining Φ= 38+28/60+12.6/3600 = 38.470162 latitude;
Here are $\boldsymbol{\delta = 4.61197}$º ve **$\Theta_z$ = 43.459°** values are found.

Using Appendix 3, it is found at an altitude of A=0 at the specified location, τ_b ~= 1,095705 and τ_d ~= 0,322027. Finally, using (2.9), (2.10) and (2.11), it can be calculated as I_{cthz}= 1038,35 W/m^2 .

2.5 Solar Tracking Systems

In solar energy applications, the amount of energy reaching the receiving surfaces depends on the cosine value of the angle of incidence of the solar beam. When the solar beam come at a right angle to the receiver surface, it will produce the maximum energy. Figure 2.8 shows single-axis and dual-axis solar tracking system designs (Alata, Al-Nimr, & Qaroush, 2005).

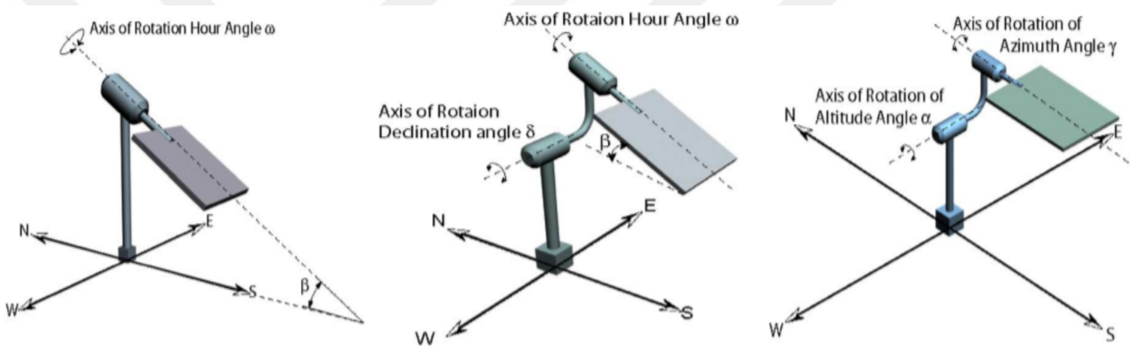

Figure 2.8 (From left to right) One-axis sun-tracking system with tilt angle equal to the latitude angle; two-axis equatorial sun-tracking system with tilt angle equal to latitude angle; two-axis azimuth/elevation sun-tracking system.

Solar tracking systems provide efficiency advantages compared to systems with fixed receiving surfaces. In the case of photovoltaic panels, studies have been conducted showing that this efficiency advantage reaches 33% (Gay, Yerkes, & Wilson, 1982).

The first study on the solar tracking system was carried out by (Finster, 1962) with the mechanical working principle. Saavedra, (1963) on the other hand, proposed a mechanism with electronic control for the first time. He used the mechanism to orient his Eppley pyrheliometer in his work.

Since those years, studies have been carried out that examine solar tracking systems from different aspects and offer original solutions. The studies can be basically considered as active and passive systems. Active systems are systems that direct the receiving surfaces to the sun with engine and gear systems. Passive systems, on the other hand, are systems that direct the receiving surfaces to the sun by using compressed gas or liquid at certain pressures and conditions (E. Anderson, Dohan, Sikora, Bitar, & McNeill, 2003; Clifford & Eastwood, 2004; Elmaged & Kamal, 2015; Gevorkian, 2010). Although there are many studies on passive systems, since the trend in tracking systems is for active systems, in this study, classification will be made according to the number of axes, tracking strategy, control method and drive method.

2.5.1 Solar Tracking Systems Based on Number of Axes

Solar tracking systems are used as single-axis and dual-axis depending on the number of free axes they have. Dual-axis systems are capable of following the seasonal movement of the sun as well as the daily movement.

While single-axis tracking systems are simpler, dual-axis systems are more complex and expensive. However, both types of systems are in demand. It should be stated that dual-axis systems are superior to single axis systems in terms of the efficiency they bring in production despite their costs during installation.

2.5.1.1 Single Axis Solar Tracking Systems

Single axis solar tracking systems are systems that track the sun with a single axis movement. They perform this movement in the East-West direction, in an inclined position, with azimuth tracking (vertical axis).

N. H. Helwa, A. B. G. Bahgat, A. M., (2000) examined four different systems, fixed system, vertical axis azimuth tracking, North-South inclination system, double-axis system tracking azimuth and elevation angles, on which photovoltaic panels were placed in their study. All systems are controlled by microprocessors and monitored throughout the year. It has been observed that the most solar radiation is collected in the system with dual-axis azimuth-elevation tracking, so the highest energy output is in this system. In addition, information on single-axis systems has also emerged. It was observed that the vertical axis azimuth tracker obtained the most energy output after the dual-axis tracker system. It has been stated that the inclined single-axis tracker system produces more energy in summer than the fixed system, on the contrary, it is lower than the energy production of the fixed system in winter.

Kim, Han, & Seo, (2008) investigated the thermal efficiency of single-axis solar tracking in the Compound Parabolic Concentrator (CPC) system. They compared the data they obtained through calculations with the measurements. It was noted that the thermal efficiency increased by 14.9% and was more stable when the tracking system was used.

Poulek & Libra, (2000) proposed a system in which they control bifacial solar panels directly with a DC motor with a unique, simple mechanism. Thus, they have realized a design that can find application in space systems, in which bifacial panels are used.

In their study, Mavromatakis & Franghiadakis, (2008) designed a special system in which they can direct the collector in two directions with special supports. It is stated that the system behaves like a dual-axis system and similar results are obtained.

2.5.1.2 Dual Axis Solar Tracking Systems

Dual-axis solar tracking systems aim to increase efficiency by tracking the daily and seasonal movements of the sun in the sky. In the proposed systems, the azimuth angle (γ_s), altitude (α_s) angle or zenith angle (θ_z) is obtained and the photovoltaic panel or thermal receiver surface to be placed is positioned to overlap these angles.

Abdallah & Nijmeh, (2004) compared a two-axis sun tracking system with a system fixed at 32° inclination in their study. They implemented the proposed system with PLC to control the β tilt angle and azimuth angle. It has been observed that the energy produced is 41.34% more compared to the fixed system. Kivrak, Gunduzalp, & Dincer, (2012) compared the fixed system and the dual-axis tracking system they constructed in their study. They recorded the energy produced by placing the fixed system with an inclination of 37°. In addition, they compared the energy obtained from the dual-axis system, which they controlled the azimuth and altitude angles, and the theoretical outputs obtained by computer simulation. In their study, they found that the tracking system produced 64% more energy compared to the fixed system.

Maatallah, El Alimi, & Nassrallah, (2011) compared the fixed system and the dual-axis tracking system in detail in Mostari City. Full-day data were analyzed at the spring, summer, autumn and winter solstice times. According to the results they obtained, energy production increased by 30% at the winter solstice and by 44% at the summer solstice.

2.5.2 Solar Tracking Systems Based on Tracking Strategies

When the tracking approaches of solar tracking systems are evalueated, there are some prominent strategies. These are strategies that utilize time and date information, utilize microprocessor and optical sensors, and a combination of these.

2.5.2.1 Tracking Systems Based on Date and Time

These tracking systems fulfill these tasks by utilizing the date and time information of the system, geographical information, and astronomical equations.

Davies, (1993) proposes a second axis perpendicular to the elliptical plane in his study. With this system, which provides ease of control with constant speed applied to the actuators, it can track the sun with an error of +/-2°. Edwards, (1978) carried out his work with solar parabolic collectors. Using the time information, he operated the actuators that directed the collectors at different speeds at different times of the day. In his computer-aided study, he emphasizes that appropriate speeds should be set for each collector's actuator.

Blanco-Muriel, Alarcón-Padilla, López-Moratalla, & Lara-Coira, (2001) applied the solar tracking systems they developed in high-density thermal solar collectors in their study. In the study, an alternative to the existing algorithms, more efficient and effective working algorithm has been developed. This algorithm uses time, date and geographic location information as input information. It is stated that the study provides efficiency and ease in computational capacity.

In his study, Thomas, (2017) creates the sun tracking angles with the help of the computer program he developed visually. Using astronomical equations and time and date information, he obtains the azimuth and elevation angles of the sun in the sky for different geographical locations.

2.5.2.2 Tracking Systems Based on Optical Sensors

Tracking systems designed using optical sensors benefit from the optical properties of the sun. These can be properties such as the amount of radiation from the sun, the angle of incidence of the solar beam, the effects of shading on the surfaces.

Lynch & Salameh, (1990) performed sun tracking by using two sensors together in their study. The first of the sensors consists of 4 solar cells placed on a pyramid-shaped structure. The main purpose of the system was to minimize and equalize the difference between the values read from these 4 sensors. The second sensor is tilted to the south direction. The purpose of this sensor is to eliminate errors caused by initial condition and diffuse radiation. Electronic control circuits in which these two sensor structures are controlled have been designed and azimuth and zenith motors have been driven. It is stated that this low-cost system can find application area in large-scale systems.

Koyuncu & Balasubramanian, (1991) directs the solar panel in the East-West direction with 4 LDRs placed in the tracking system they developed. In this study, similarly, the values read over LDRs were interpreted differentially. The motor is directed in the area determined by the limit switches with the developed simple algorithm.

S. A. Kalogirou, (1996) used 3 LDRs together in a single-axis tracking system in his study. The first of these enabled the collector to focus, the other the cloud cover in the sky, and the last to obtain day/night information. Although no clear value is given for the tracking error in the system controlled by analog circuit, it is stated that it will be below 5°. Abdallah & Nijmeh, (2004) controlled the system in which they collected information about the position of the sun with the help of photosensors with PLC in their study. They planned the software in this way by dividing the day into 4 different time periods. In the study, a 41.34% increase was obtained in the daily collected energy compared to the fixed panel with 32° inclination.

2.5.2.3 Tracking Systems Based on Combination of Tracking Strategies

When the studies are considered in terms of tracking systems, it is encountered with studies that combine some methods and techniques. It is seen that these studies are generally used to increase the accuracy and stability of the system and to verify the results obtained. In their study, Ajay & Nagaraju, (2003) created a single-axis tracking system that obtained day/night information and sun direction information with LDR pairs. In addition, the microcontroller circuit they established communicates with the Real Time Clock (RTC) IC. Thus, the microcontroller calculates the position of the sun by interpreting the information coming from the sun sensors and the information coming from the RTC in order to generate the signal to be transmitted to the motors. It is stated that with the study, results were obtained with a resolution of 1° without being affected by clouding in the sky.

Luque-Heredia, Gordillo, & Rodriguez, (2004) designed a tracking control system that also includes error sources and error estimations. In this system, error sources, error estimations and sun position calculations, which are subjected to a model validation, are used together. Data from sun sensors were also used for feedback. Similarly, Rubio, Ortega, Gordillo, & López-Martínez, (2007) used open loop control and feedback control together in their study. In open loop control, tracking signals are generated for the motors by using solar equations, and the tracking error is read with the help of solar sensors and feedback control is performed. In this study, in which they combined two different operating modes as a hybrid, it is stated that there is benefit compared to operating in a single mode.

In the study of Al-mohamad, (2004), photosensors, day and date information and PLC units were used together. The system working according to the algorithm he developed was compared with the fixed system. Compared to the fixed system, 20% more energy was produced and it was monitored on the computer by means of serial channel communication. Thus, it is stated that the initial cost disadvantage of tracking systems is a cost-effective study, and it is stated that it actually has a cost-reducing effect.

C. D. Lee, Huang, & Yeh, (2013) used the image of the sun in their study. A camera was used to obtain the image of the sun, and then image processing techniques were used. In order to prove the accuracy of the sun sensor and the image processing-based embedded controller, a platform where the image of the sun is tracked has been established and its performance has been tested. The proposed solar tracking system has overcome the stability problem in cloudy weather conditions and has reached an accuracy of 0.04˚. In the study, firstly, Cassegrain telescope and camera, which they designed themselves, were used to obtain a clear and large enough photo of the sun. If the sun photo taken is too small, uncharacteristic noise and errors will appear in the photo due to numerical processing, making it difficult to filter out and estimate the sun's center. A software called OSLO Tool (Research, 2010) was used to analyze the characteristics of the designed telescope. The MTF (Modulation Transfer Function) of the telescope was obtained from this software. Thus, it has been understood that the designed telescope has good contrast. A number of image processing techniques have been applied to the image, which has been acquired sufficiently large and clean. After processing, the Sobel method (Vincent & Folorunso, 2009) was used to determine the circular borders of the binary image. When sun tracking is done correctly, the center of the sun circle in the image frame should coincide with the center of the image. In order to approximate the center of the obtained sun circle to the image center, it was necessary to obtain the equation of the circle. With the help of the 3-point circle method, the equation of the circle is obtained by using 3 points on the circle. By shortening the calculation, the relationship (x_1,y_1), (x_2,y_2), (x_3,y_3) can be obtained, which will directly obtain the coordinates of the image center (x,y). In the rest of the study, it is mentioned that the image-based sun sensor provides the sun's orbit and this creates an opportunity to test the performance of the sun sensor. In addition, some comparisons examining the tracking errors were made and the accuracy of the proposed system was demonstrated.

Abdollahpour et al., (2018) used the optical properties of the solar beam in their study. The shadow formed on the surface by the effect of the sun on the rod placed perpendicular to a surface on the panel has been studied. The length of this shadow and the slope of the shadow provide information about the orientation of the solar panel. This image of the shadow taken with the camera was processed with image processing techniques, and with the help of linear regression methods, relations were established between the center point of the shadow and the farthest point of the shadow. It is stated that with the study, 2 ˚ accuracy sensitivity is obtained in sun tracking.

Garcia-Gil & Ramirez, (2019) designed and implemented a sun tracker based on panoramic images taken with a fisheye camera in their study. The captured images digitally estimate the azimuth and altitude angles of the sun. The estimation process is based on correlating the image taken with the fisheye camera to geographical locations and then determining the center points in the part where the sun is located. The estimated angles are collected in the microcontroller, which manages the sun tracker positioned with the help of the accelerometer and gyroscope. The proposed system works satisfactorily regardless of whether the weather is sunny or not.

Carballo, Bonilla, Berenguel, Fernández-Reche, & García, (2019) is a study in which a low-cost alternative to traditional methods, solar tracking with computer vision and deep learning is developed and tested with open source hardware. The tests and the overall study were conducted at Plataforma solar de Almeria (PSA) in Spain. With the system, one of the goals is to direct the solar beam to the central tower with the help of heliostats in the solar field. The proposed system can provide the key parameters of cloud motion tracking, obstacle and shadow detection, atmospheric attenuation or solar radiation measurement in order to develop strategies that will increase system performance in sun tracking. The neural network model used in the study is a model that produces an output (object locations) to an input (image) similar to other models. In addition, iterative processes called learning and training are also run. Training is an optimization problem and tries to minimize the loss function. The aim is not only to minimize the difference between the predictions and the datasets used in training, but also to generalize to previously unseen examples.

2.5.3 Solar Tracking Systems Based on Control Methods

The preferred tracking system directly affects the energy output in all solar energy applications. In terms of the control methods used in solar tracking systems, it is seen that the systems are designed according to open loop or closed loop methods. Although high-efficiency results are obtained with both methods, advances in control theory in the last twenty years have contributed to the development of closed-loop solar tracking systems and making them more efficient than open-loop systems.

2.5.3.1 Open Loop Solar Tracking Systems

When sun tracking is performed with open-loop control systems, the system created can be used with various calculation methods, astronomical equations, sensors, etc. It directly applies the outputs of the sun's position, does not support it with any feedback system. In this sense, simpler applications can be made compared to closed-loop controls.

Al-Naima & Yaghobian, (1990) implemented a passive 2-axis tracking system in their study. They electronically controlled the tracking system they created according to the astronomical coordinates of the sun with mechanical gear systems. It is stated that at the time of the study, higher precision results were obtained than conventional sensor-controlled systems. Reda & Andreas, (2004) used an algorithm using zenith, azimuth and incidence angle in their work to create an open loop control solar tracking system. In order to obtain highly accurate results, parameters such as elliptical latitude and longitude, equinox dates, declination angle were used in their calculations. Their work has ensured that an accuracy of 0.0003˚ can be achieved.

Chen, Feng, & Hong, (2006) developed an open-loop solar tracking system with their digital sun sensor. In their algorithms, they used the nonlinear measurement principle, in which the projective image of the incoming sun rays creates a control signal with 4 quadrants. They also tried to compensate for the errors that may arise with mathematical formulas. It is stated that the accuracy value of 0.2˚has been reached with the study.

Grena, (2008) obtained high-accuracy results regarding the position of the sun with an efficient algorithm when compared to algorithms based on other astronomical calculations. By using latitude, longitude, time date information, hour angle, azimuth, zenith, atmospheric losses correction values were obtained. Angular accuracy of 0.0027˚was achieved without the need for a closed-loop control system. It is envisaged that a 20-year operational period of the system has been validated. Similarly, Chong & Wong, (2009) obtained a mathematical formulation in which azimuth-elevation and tilt-roll tracking were carried out, and high accuracy results were obtained. This formulation is derived through coordinate transformation and it provides solutions especially for installation errors.

Yang, Cheng, Cheng, Wang, & Lee, (2017) developed an open-loop controlled, easy-moving, stand-alone altitude-azimuth tracker in their study. In the study, there are both the collector focused by the fresnel lens and solar panels. The purpose of adding a solar panel to the system is to obtain the energy that will move the motors from the system itself. The Stirling motor is placed at the point focused by the lens. The importance of the thermal conductivity of the liquid used at the points where the heat is collected and the isolation of the Stirling engine receiver surfaces are demonstrated by the study.

2.5.3.2 Closed Loop Solar Tracking Systems

Closed-loop solar tracking systems are based on the feedback principle established with various sensors. The outputs produced by manipulation and calculations using the data obtained from the sensors are applied to the tracking system. Closed-loop control systems can be characterized as systems that are more open to development since the systems themselves can work to reduce the error rate.

Alorda, Pujol-Nadal, Rodriguez-Navas, Moià-Pol, & Martínez-Moll, (2015) made precise positioning over the CAN network in which solar collectors are individually controlled. In the control system they use, the information received from the radiation sensor and encoder is used as feedback. Thus, the system becomes more convenient for supervision and maintenance.

Delgado et al., (2012) designed, produced and characterized a sun sensor in their study. They used two structures with two mirrors that reflect sunlight. Closed-loop control is preferred in both systems. While the target point reflected by the mirror is measured in the first, one of the two sensors used in the second one measures the position of the sun and the other measures the position of the sun on the mirror plane of the sun. In the system installed for lighting purposes, the sensor information in question is interpreted and it is stated that the system works with an accuracy of 0.1˚.

Da Rocha Queiroz, da Silva Souza, Gussoli, de Oliveira, & Andrade, (2020) developed a two-axis closed-loop solar tracker prototype in their study. Algorithm outputs forming the angular reference are applied to the driver circuits with the hysteresis on/off controller. Driver circuits also control the physical system. Angular position information is taken as feedback in the system, and a comparison is made with the angular reference values created at the initializing . It is stated that the accuracy value increases in both angles with the system and the energy output increases compared to the system using fixed solar panels.

Zhou, Chen, Hu, Nie, & Wen, (2021) placed a Stirling engine in the center of the solar system in the form of a dish. The control of this system in elevation and azimuth angles was realized with PLC. Inclinator and encoder were used as feedback for these two angles. In the system where the information from the feedbacks is interpreted by comparing the desired angular values, the amount of angular error can reach 0.278˚in azimuth and 0.321 ˚ in elevation. With the applied closed loop control, these high accuracy values have been achieved.

2.5.4 Evaluation of Solar Tracking Systems Literature

Many studies have been carried out according to the number of axes, tracking strategy and control methods related to solar tracking systems. When these studies are examined, it is seen that each of them contributes to academic studies according to the tracking method and they are beneficial from different theoretical and practical perspectives. However, it is seen that certain expectations from tracking systems have emerged.

Angular accuracy is what is primarily expected from solar tracking systems. The majority of the studies carried out supported their studies with angular accuracy values and verified their own systems in this way. Considering that angular accuracy has a direct effect on the total energy output obtained, its contribution to total efficiency and its importance in studies can be understood.

Another important issue in terms of solar tracking systems is the durability of these systems and their ability to continue to work under conditions of various environmental factors. These include conditions such as climatic events, shading and cloudiness. This is due to the fact that it is an issue that directly affects the daily, weekly and annual production values of the systems.

Since solar tracking systems affect both installation and commissioning processes, it is an important parameter whether they are simple or complex in design. In this context, both mechanical and electronic parts are mentioned. The mechanical complexity of the systems affects the proper operation of the actuators used, and is also important in maintenance and failure issues. Electronic parts are also important for reasons such as the need for computational capacity, required computation times, and efficient use of electrical energy.

Another important issue for solar tracking systems is the cost issue. These systems are costly systems when considering the design, installation and commissioning processes. However, studies show that solar tracking system investments are cost-effective investments. With the total benefit solar trackers provide, they can recover their investment costs in a short period.

CHAPTER THREE

SPHERICAL SENSING OF THE LIGHT SOURCES AND DEVELOPED SENSOR

3.1 Spherical Sensing of The Light

The light emitted from the light sources to the environment propagates linearly. The sensors, which measure both the optical power and the light intensity of the light, can be positioned according to the Cartesian coordinate plane. If a unique measurement technique is not created according to the angle of incidence of the light in the internal structure of these sensors, they can only detect the physical properties of the light in one axis. However, this information is not sufficient to determine the exact location of the light source. The number of sensors should be increased as needed by the axes in the coordinate system.

Transformation can be made from the Cartesian coordinate system to the spherical or polar coordinate plane when necessary. These three most commonly used coordinate systems are shown in Figure 3.1.

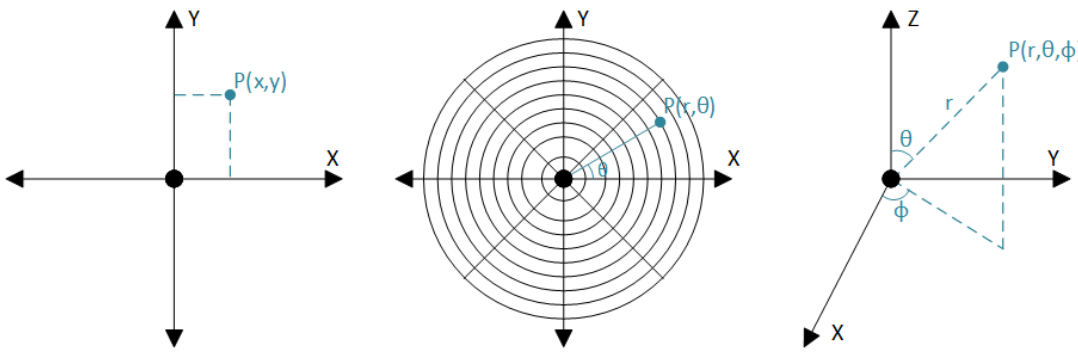

Figure 3.1 Cartesian, Polar and Spherical Coordinate Systems (left to right).

The point P(x,y) expressed in the Cartesian coordinate system is expressed as $x = r.\cos\Theta$, $y = r.\sin\Theta$ as a result of the geometric inferences of the relationship seen in Figure 3.1. The point P(x,y,z) in the spherical coordinate system is also expressed as $x=r.\sin\Theta.\cos\varphi$, $y = r.\sin\Theta.\sin\varphi$, $z = r.\cos\Theta$.

The need for transformation between coordinate systems necessitates the need for a continuous transformative calculation to interpret the information read from the sensors. In this context, if the sensors are placed directly on a solid object suitable for the coordinate system to be transformed, instead of a Cartesian plane, the data read will be directly compatible with the coordinate plane of the solid object in question and do not require transformation. In this context, point sensor arrays placed in a spherical order can be seen in Figure 3.2. In the figure, examples are created with varying sensor numbers according to different θ and φ angular intervals.

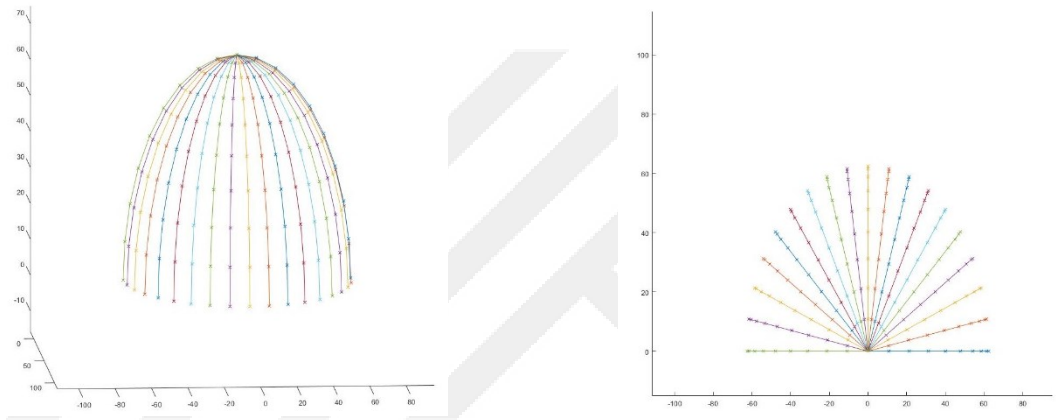

(a)

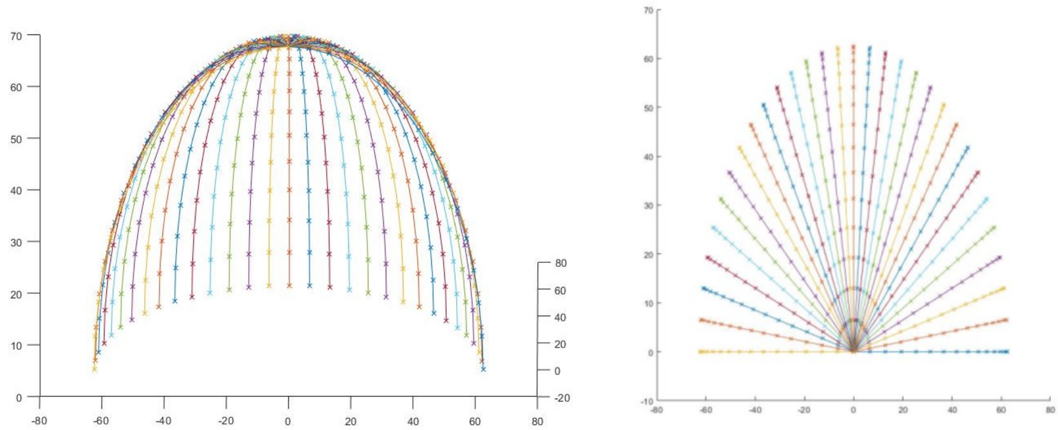

(b)

Figure 3.2 Hemispherical point placement with angular intervals of 10˚at angles Θ and φ (a). Hemispherical point placement with angular intervals of 6˚at angles Θ and φ (b).

As seen in the examples in Figure 3.2, the shrinking of the angular intervals increases the resolution of the spherically received data. In Figure 3.2.(a), a total of 9 sensors can be placed in the direction of the ϴ angle and a total of 18 sensors in the direction of the φ angle can be placed for a hemispherical sphere with 10° intervals. In Figure 3.2.(b), a total of 15 sensors can be placed in the direction of ϴ angle with 6° intervals, and a total of 30 sensors in the direction of φ angle.

3.2 Benefits of Spherical Sensing

The spherical sense of light sources creates data in the spherical coordinate system thanks to the placement positions of the light sensors in the spherical model. These data provide great convenience for the localization of the light source in the 3D physical world. This eliminates the need for any transformation. When transformation to the desired coordinate system is required for different applications and studies, this process can also be performed. The elimination of the need for transformation between coordinate systems also reduces the microprocessor calculation capacities required for this process. In this context, it is possible to localize light sources by using energy effectively with low processor capacities.

3.3 Sensor Model

A sensor model was developed considering the advantages of perceiving light spherically. In this model, light sensors, which are considered as point, are placed at ϴ and φ angles with 30° angular intervals. Sensor locations are shown in Figure 3.3 with polar coordinates.

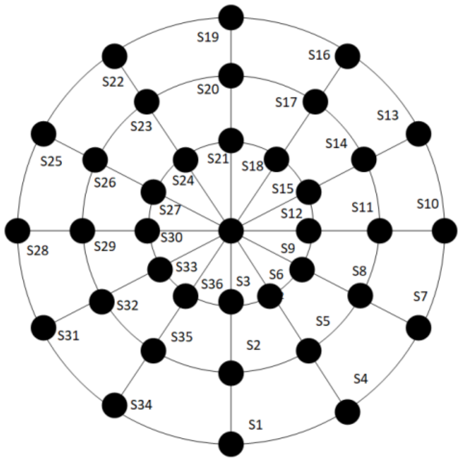

Figure 3.3 Sensor Placements in Polar Coordinates.

In the Φ azimuth angle direction – if it is expressed in terms of sun angles - the sensors arranged in order S_1, S_4, S_7, … S_{34} can collect data from a total angular width of 360° with 30° angular intervals. In the Θ elevation angle direction – if it is expressed in terms of sun angles – the sensors are lined up as (S_1, S_2, S_3, S_{37}), (S_4, S_5, S_6, S_{37}), … (S_{34}, S_{35}, S_{36}, S_{37}) with each sensor array. Due to the semispherical structure, data can be collected from an angular width of 90 °.

3.3.1 3D Model

In the semispherical body where the sensors will be placed, 3D design has been carried out according to the criteria determined in the model. Optimum conditions are provided by taking into account the dimensions of the sensors to be placed as r=2.5 cm according to the spherical coordinate plane in the design. Figure 3.4 shows the 3D design.

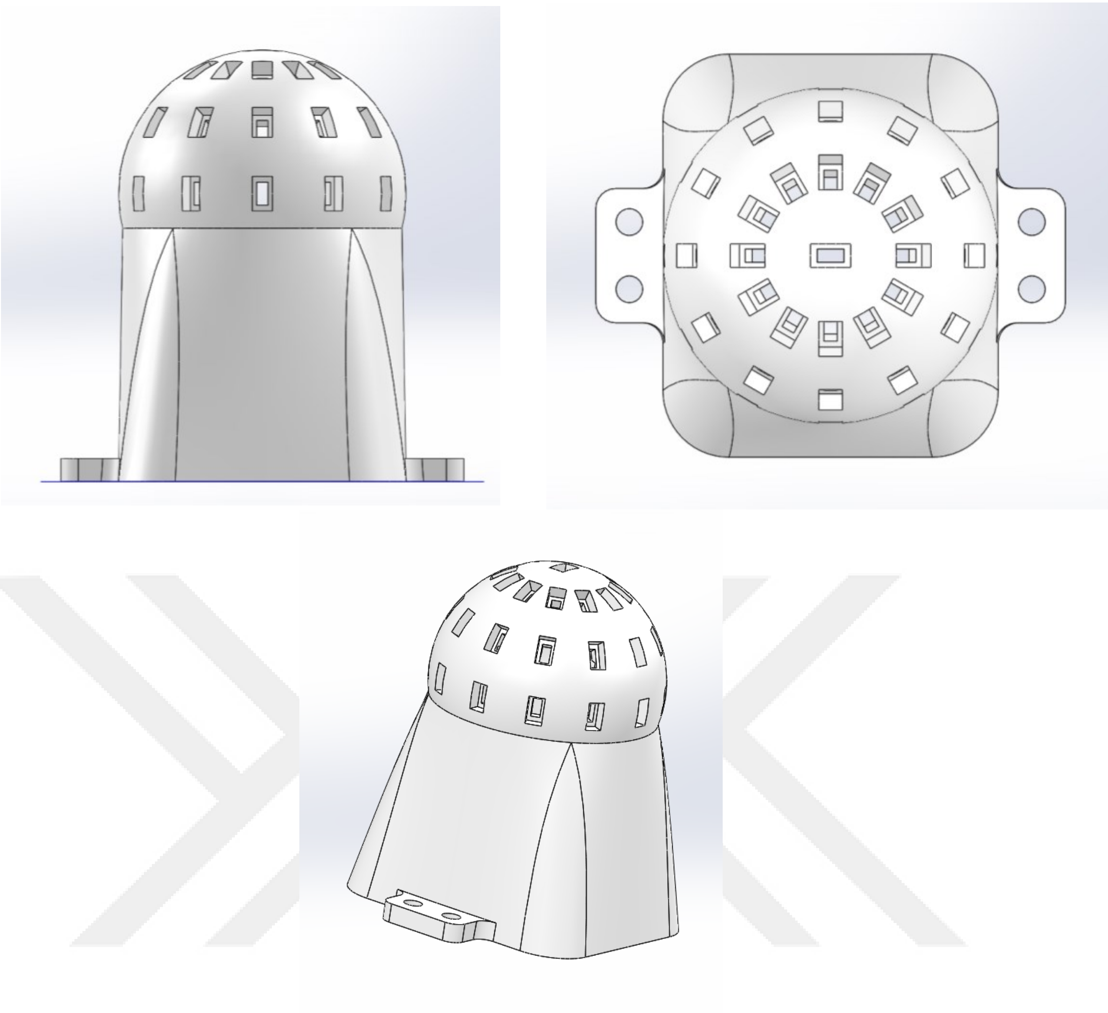

Figure 3.4 Designed 3D Model of Semi-spherical Structure.

3.3.2 Developed Model

In recent years, high impact of additive manufacturing (AM) or 3D printing technologies in general has become apparent. Thanks to AM technology, localized, customizable productions of the objects rather than mass production and transportation are made possible. Thus, such parameters as cost and time can be saved on to a considerable extent AM technology also provides novelties for industrial components that have been traditionally produced. These components, about which common knowledge regarding the mechanical design are already known, can be reproduced with different materials in a customized way (Klassen et al., 2012; Vaezi, Seitz, & Yang, 2013). Or, current designs can be updated with brand new features with the addition of circuit components (Gräbner, Dödtmann, Dumstorff, & Lucklum, 2018). Besides, AM technology contributes to sensor production as well. It is seen in the conducted studies that this technology made contribution in such fields as electrical, thermal conductivity, radiation protection, flow, force and pressure measurement (Dijkshoorn et al., 2018; Lucklum & Dumstorff, 2017; Miner, Ham, & Kluitenberg, 2017; Saari et al., 2016). This contribution is made by enabling production in different geometries, being easily customizable and used in microscales.

In this study, CAD model designed semi-spherical body is produced by using AM technology. For the light sensors, gaps, are created on the semi-spherical body in horizontal and vertical directions and with 30° angular distances to enable the sensors to fit in.

Solidworks is used for model design while Ultimaker Cura softwares are used for model slicing and printing preparation. It is created with FDM (Fused Deposition Modeling) type 3-D printer (Ender 5 Pro) having 0.4 mm Nozzle diameter and by using Polylactic Acid (PLA) as the printing material. Layer filling speed is arranged as 25 mm/s and appropriate printing and plate temperatures are chosen as 208 C◦ - 70 C◦ respectively. By taking into consideration the printing quality, printing is completed with the help of supportive structures. In post-processing phase, supportive structures required for the printing are taken apart and the printing is cleaned up. Rasping is applied manually on a limited extent.

Diameter of the model hemisphere is 50 mm, inner thickness for the sphere is 5 mm and for the part into which the sphere is placed is 10.92 mm. Inner part of the hemisphere is left empty. In this way, enough space to place the sensor cables onto the circuit cards is acquired. The body is affixed to the circuit box underneath with screw holes on both sides to make the body stable and balanced during the measurements. The body created based on the designed model and used during the rest of the study is shown in Figure 3.5.

Figure 3.5. 3D Printed Model.

3.3.3 Electronics Implementation

Light sensors are placed on the body in order to collect data about the light source from the body produced. With the proper connections, the data read from the light sensors have been transferred to the designed electronic circuits. Thus, appropriate steps were taken to interpret the incoming data.

The visualization of the received data and its use according to fuzzy logic rules are explained in the following parts of the study. Figure 3.6 shows the schematic of the applied measurement system.

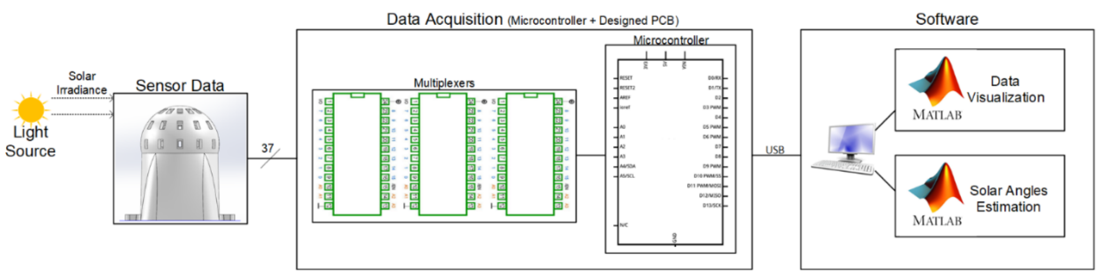

Figure 3.6 Schematics of The Applied Measurement System.

The schematic representation of the whole PCB design and the designed PCB layout are in Appendix 4. In addition, the program codes in which the sensor data are measured and transferred to the computer environment via serial channel are included in Appendix 5.

3.3.3.1 Light Sensor and Its Features

In solar tracking studies, LDRs can be used to understand the position of the sun in the sky. In these studies, LDR's are placed in specific positions in a way to represent the geographical directions with various methods. In this way, although it is possible to track the sun using LDRs, it is seen that the results are within certain limits and angular outputs cannot be obtained. In this study, LDR's that yield limited information on sun's position aren't used. Instead, TEMT 6000, a photo-transistor sensitively working especially on the visible wavelengths, is used as the light sensor. Thus, electrical current can be obtained with a linear curve in accordance with Lux, the luminous intensity unit emerging in the light sensor. These light sensors exhibit the sensitivity peak point value at 560 nm and the range of spectral bandwidth is 360-970 nm (Vishay Semiconductors, 2004). Concordantly, sun's solar spectrum emits a major part of its energy in the visible light range of 350-750 nm (Messenger & Abtahi, 2017). These values show that the measurements made by means of these light sensors are appropriate to use of detecting the light emitted by the sun in the sky.

Designed and produced PCB and the electrical diagram of the sensor, which is measured by placing 37 pieces on the body, are shown in Figure 3.7.

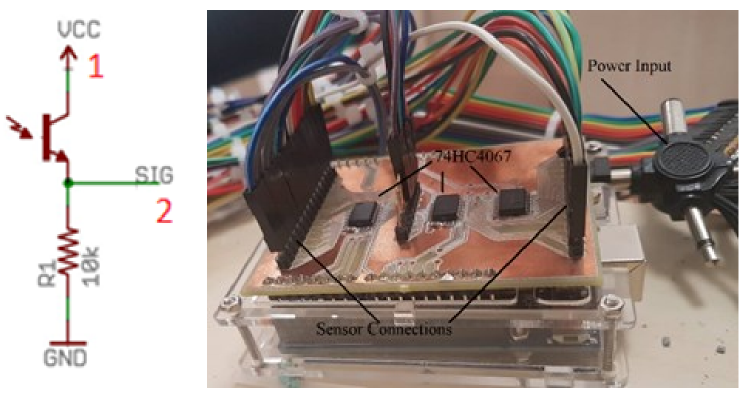

Figure 3.7 Electrical Diagram of TEMT 6000 and Produced PCB.

3.3.3.2 Multiplexers and ADC Conversion

Multiplexers are circuit elements that transfer the information contained in the input to the output terminals with the help of selector terminals operating as analog or digital. In the study, analog multiplexers were used to collect data from 37 different sensors. Necessary selective terminals are controlled by microcontroller and read by analog input terminals of microcontroller. There are 10-bit Analog Digital Converters (ADC) at the analog terminals of the microcontroller. With this method, the voltage ranges read between 0 and 5 V are converted into numerical values between 0 and 1023. Reading from the sensors is performed at high speed, and the entire sensor array is scanned.

3.4 Features of The Sensor

The sensor, in which the light is perceived spherically, creates a unique structure on its own, apart from the software created for visualization and localization. In this sense, it is a sensor where the information coming from the light sources is detected as 0 – 360 ° in the azimuth direction and 0 – 90 ° in the elevation direction, and is transmitted securely by serial channel communication. Communication speed, 2,000,000 baud rate is preferred. It has been observed that synchronization problems occur at higher speed. HEX format is preferred in order to reduce the amount of bits sent during communication. Thus, for each step value above 9, an increase in efficiency was achieved. However, in this case, there is a constant variability in terms of packet data size transferred to the serial channel, depending on the size of the read data (in cases where the light intensity increases). This problem was fixed by checking the coding.

The read data is checked before being transferred to the serial channel so that there is no missing / excess data and does not cause additional problems on the side of Matlab. The numerical control of the data transferred to the serial channel does not mean that the data is sent correctly and completely. Therefore, the data sent was checked by making a Checksum calculation. The data sent for the CheckSum account is collected and the last two digit values are taken in the HEX form and the calculation is completed by subtracting this value from the 0XFF value. It is expressed as *checksum = 0xFF- (sum & 0xFF)* in the coding. With the improvements made, a significant improvement in speed has been achieved.

CHAPTER FOUR

DATA COLLECTION AND MEASUREMENTS

4.1 Data Collection

The sensor, which sends the data from the light source by serial communication, transmits data series instantly. In the study, the data taken from the light source was used for instant localization as well as by recording. These collected data may contain disturbing effects and noises due to environmental conditions. For this reason, the Time Synchronous Average Method was used in the rest of the study, which will work as a filter that can minimize the disturbing effects.

In the TSA method, the measurements are made at the exact measurement points by using the synchronous signal, which determines the measurement period. This process can be carried out by using the time averaging method and considering the same issue in software coding. The time elapsed between the command lines measured in the coding part is important. The commands should be arranged in such a way that they are precisely detected and synchronized with the frequency determined in the synchronous signal. In the study, applied data collection method was used by adhering to these conditions.

4.2 Time Synchronous Average (TSA) Method

TSA (Time-Synchronous Averaging) method is an averaging method with low-pass filter effect to measure signals containing noise or high frequency components. Thus, the SNR (Signal to Noise Ratio) rate will increase. The TSA method is used in vibration analysis, gearbox error analysis, anomaly detection based on encoder data, and more generally in many studies using signal processing (Hızarcı, Ümütlü, Kıral, & Öztürk, 2021; Jablonski, 2021; Liang, Zhao, Lin, Jiao, & Ding, 2020; Zhang & Hu, 2019).

The TSA function where T denotes period of the signal and N is expressed as follows to represent the samples to be averaged.

$$X_{TSA}(t) = \frac{1}{N}\sum_{k=1}^{N} x(t + kT) \tag{4.1}$$

An example application is seen in Figure 4.1.

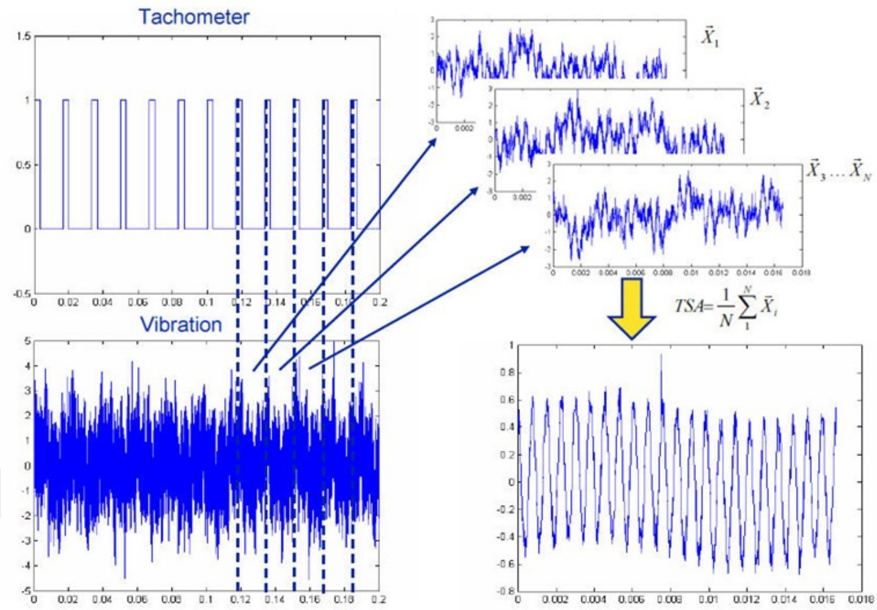

Figure 4.1 TSA Measurement in Vibration Analysis (Matlab, 2020).

The TSA method is applied on the existing sensor by analyzing it with the Profiler feature in MATLAB software. Measurements are made for 4 seconds (at 12 ms measurement intervals) at each reference point where the light source is placed. Here the synchronization signal defines the data windows time interval and can be defined by a tachometer signal or pre-defined time value. In this study data sampling time is defined as total elapsed time during complete scan of spherical sensor data. Thus, a synchronization occurs using one scan time of sensor data acquisition to get better results from time averaging. 12ms is selected as an appropriate data window size and total 4 seconds of data used for TSA method. Processed time averaging data are presented in Section 4.5.

4.3 Manual Data Collection Technique

The data created by the light source on the sensor body in this study are obtained by non-automatic positioning to certain sun angles.

Azimuth and elevation angles are the solar angles used for determining the sun's location in the sky. Azimuth angle (φ) states the angle that is formed by the sun's position and the geographical north while the elevation angle (θ) points out the angle that the sun forms with the horizontal plane. The relationship of the sun in the sky with the observer reference point is shown in Figure 4.2.

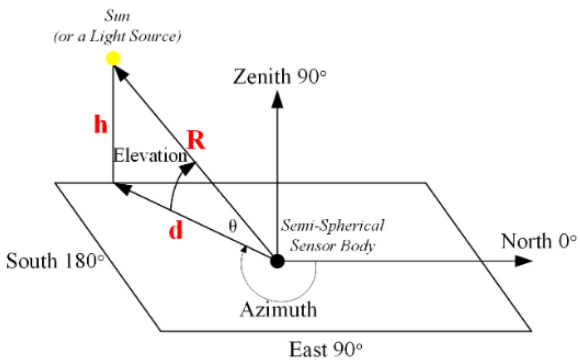

Figure 4.2. Relationship between sun and reference point.

Proposed measurement system is tested in the experiment environment and measurement values that are corresponding to the reference values are aimed to be obtained. Artificial light source is used in the experiments conducted and location of the light source is changed and thus, measurements are maintained and recorded. Subjects paid attention to regarding the experimental setup design and some key points are as follows:

- On condition that the measurement system remains at the fixed position, the measurements are made by moving the used light source in azimuth and elevation angles and with 30° angular distance. The measurements are made for 37 different locations in total.

- The distance between the measurement system and the light source (d) is fixed at 40 cm value. The reason is that h and d values increase more than necessary depending on the elevation θ angle value.

- Required h, d, R parameters are calculated with the trigonometric features in the measurements and they are determined by using lasermeter in each measurement. The direction of the light source is controlled with a lazer. Thus, erroneus measurements are avoided despite the fact that the light source is manually placed at the elevation and azimuth angles.

- Semi-spherical body and the electronic box used in the measurement system are placed in a way to enable independent movement in azimuth direction. By designing the experimental setup in this way, angular rotation of the measurement system is ensured without needing the movement of the light source in different azimuth angles.

- Experimental environment is isolated from interfering and external light sources during the experiments. Figure 4.3 shows the experiment setup without isolation.

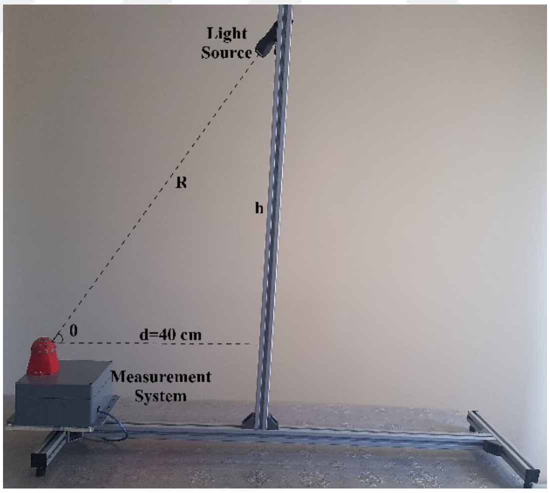

Figure 4.3. Experiment Setup.

Elevation and azimuth angles, at which the light source is located, are accepted as reference points. Measurement results yield the highest outputs mostly at around reference point or its neighbors. It is seen that the light is scattered and the sensors create approximate values with neighbor points. Samples and reference points obtained from 37 measurements are shown in Figure 4.4

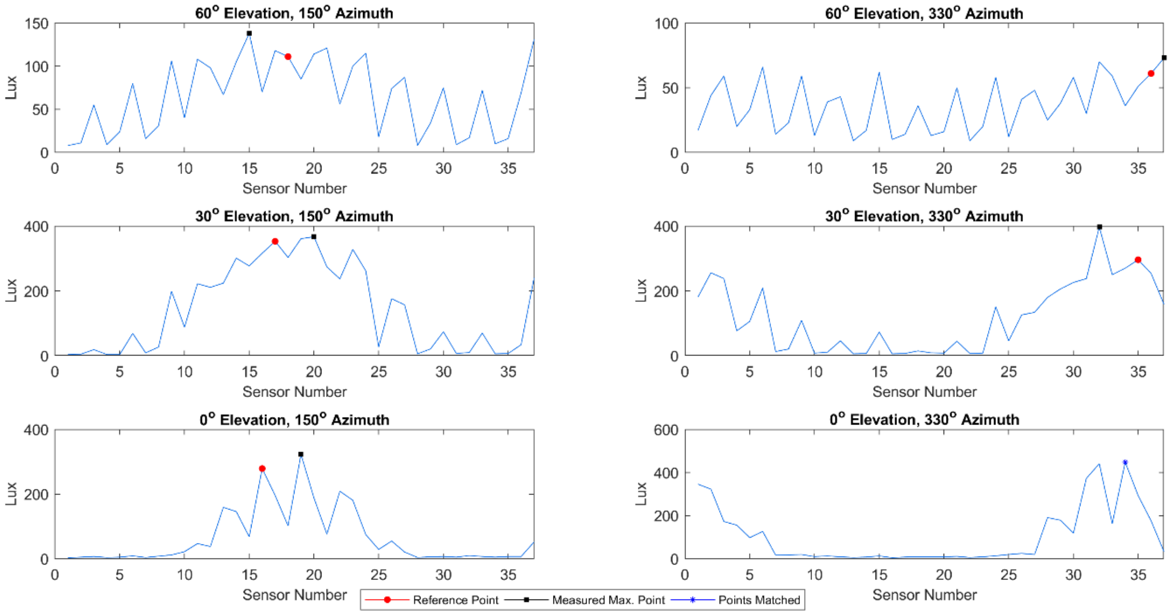

Figure 4.4. Samples of Experiment Results.

The data whose sample measurements are presented above constitute the data set to be used in the fuzzy logic algorithm in the rest of the study. In order to be used in further studies, a system capable of automatic measurement was also designed and produced instead of the existing measurement system.

4.4 Automatic Data Collection Technique

In the spherical detection of light beams scattering from the light source, the manual measurement system requires the light source to be relocated several times for each reference point. And several impractical operations are required to verify the angular positioning between the light source and the measuring system. In addition, it is a very difficult and sensitive process to create small angular differences in terms of the location of the light source. These processes can be solved both sensitively and quickly with the designed automatic measurement system.

In this system, there is a surface that is moved by two step motors that will work in the azimuth and elevation directions. The spherical sensor is placed on this surface. The smallest angular movement of the stepper motors used is 0.9 °, and the designed system can move 0-360° in the azimuth direction and 0-90° in the elevation direction. This designed and produced system can be seen in Figure 4.5.

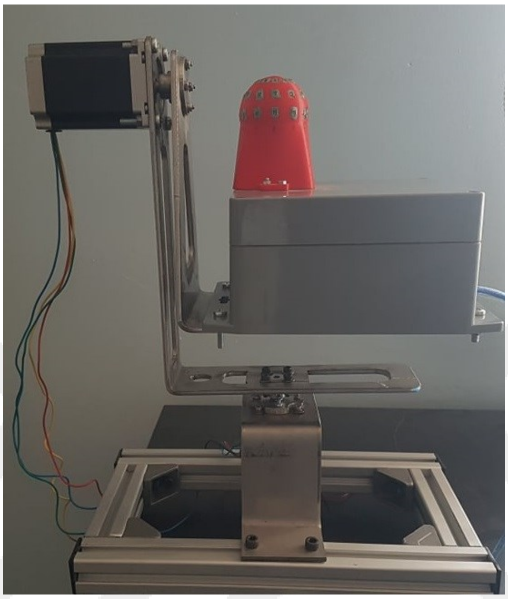

Figure 4.5 Produced Automatic Measurement System.

4.5 Sample Measurements at Angular Intervals

Sample measurements based on the TSA method were performed with a light source pointed at the reference points of the S1-S2-S3 sensors, sequently. For these 3 samples, the values measured according to the TSA method were recorded for the sensors near the reference point. These values are presented in Figures 4.6, 4.7 and 4.8.

When the presented results were evaluated, the changes between 0-9 lux values were filtered and more stable luminous intensity values were obtained. It is thought that these changes in the localization of the light source are effective in terms of accuracy.

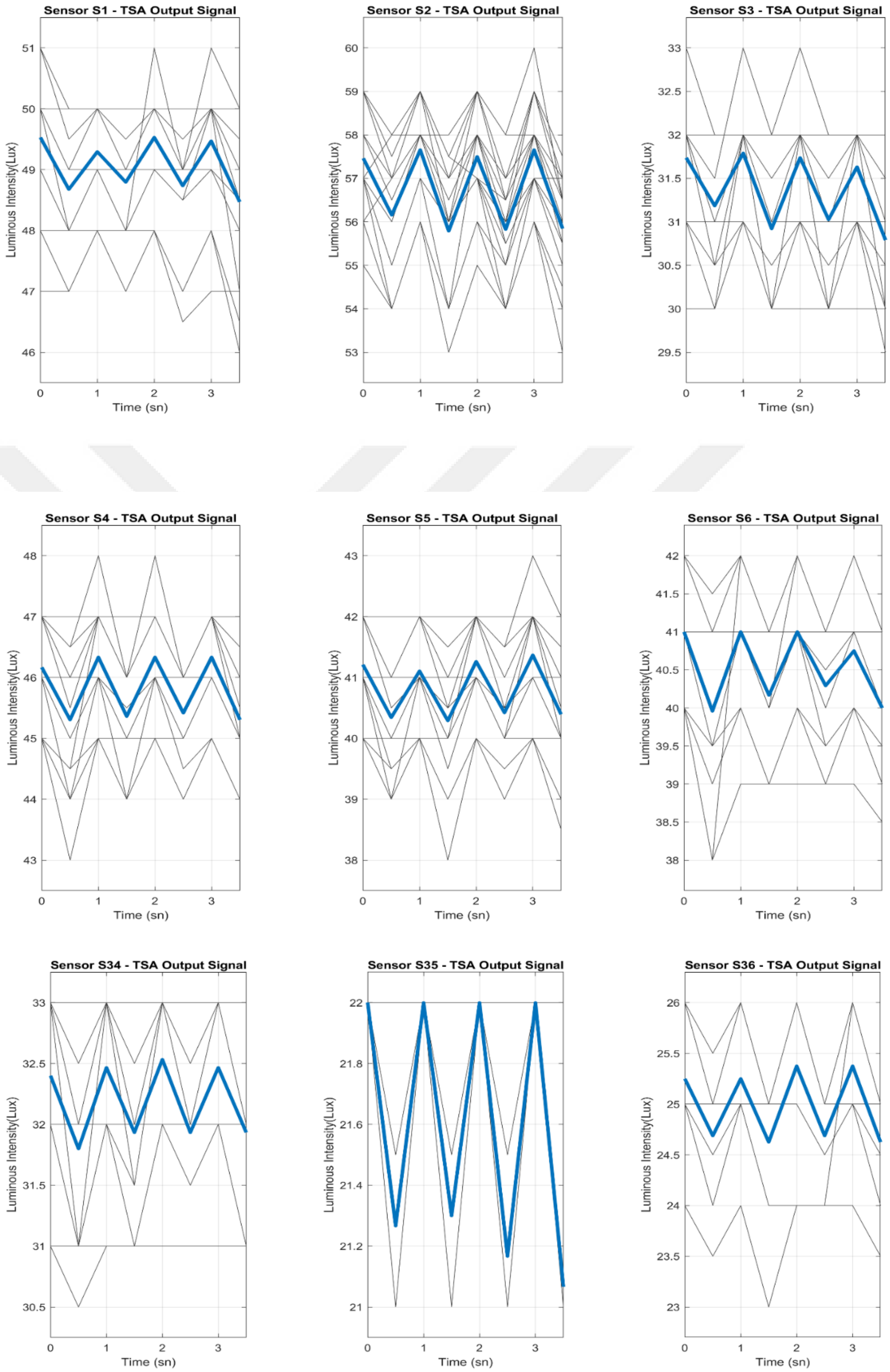

Figure 4.6 Measurement for Reference Point S1 (Azimuth 0 °; Elevation 0 °).

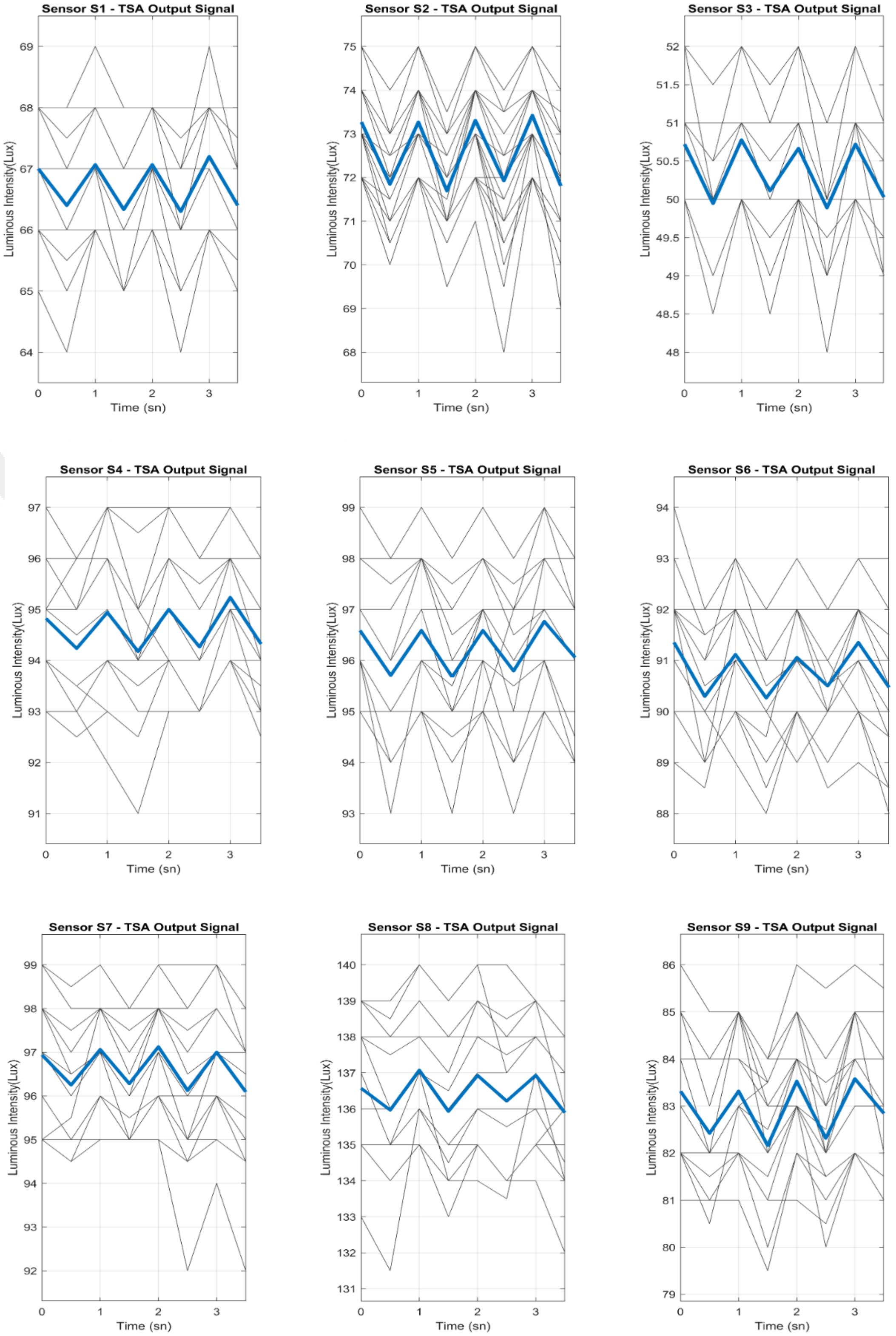

Figure 4.7 Measurement for Reference Point S2 (Azimuth 30 °; Elevation 0 °).

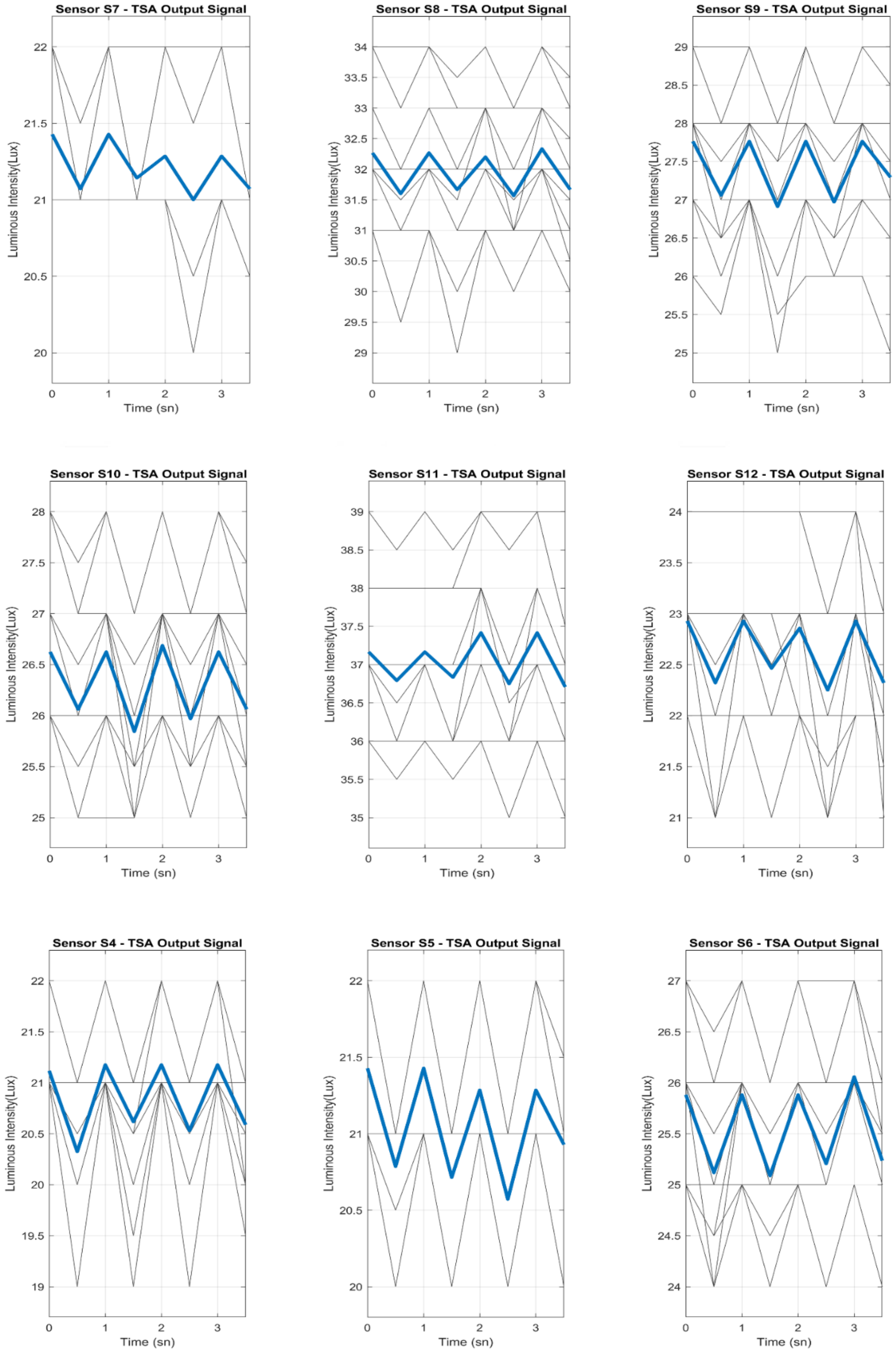

Figure 4.8 Measurement for Reference Point S3 (Azimuth 60 °; Elevation 0 °).

CHAPTER FIVE

FUZZY LOGIC APPLICATION ON DEVELOPED SENSOR

5.1 Introduction to Fuzzy Logic

The concept of fuzzy logic was first used by Zadeh from an information and control theory perspective. It is based on the fact that it replaces the theory of sets based on Aristotelian logic with the understanding of fuzzy sets. In this way, Zadeh generalized the classical set theory (Lotti Zadeh, 1965). Zadeh realized that the precise definitions of sets in classical set theory are not sufficient to explain situations in the real world, especially where model development is difficult, little knowledge of the system is available, and complexity is high. Based on this, he introduced the concept of belonging functions in fuzzy sets. Zadeh especially wanted to include linguistic ambiguities into systems. For example, we can express linguistically ambiguous expressions such as *long, short, fast, slow* in fuzzy set theory. Fuzzy logic deals with various representations of the systems in question and uses rules and membership functions in doing so (J. A. Anderson, Silverstein, Ritz, & Jones, 1977). Variables created based on linguistic values are used in the decision-making process. These values are combined with linguistic IF-THEN rules. The result of each rule is defuzzified using the membership degrees of the inputs. Expert knowledge is required in establishing rules.

5.2 Fuzzy Logic

5.2.1 Fuzzy Sets and Membership Functions

Fuzzy sets are based on a more flexible and fuzzy application of classical set logic, as the name suggests. From the point of view of classical sets valid statements are 0 or 1, true or false. However, from the point of view of fuzzy sets, it is seen that values ranged between these values are also allowed. In this respect, it can be said that it is more suitable for daily life and the physical world. Because in real life, nothing is absolutely right or wrong. In terms of fuzzy sets, except for completely true and false cases, every condition is expressed between 0 and 1 values. For example, a value of 0.8 will be expressed as 80% true, 20% false. If we consider another example, from the point of view of classical sets, old age can be defined below the age of 70. All ages below 70 years of age will not be included in the old age set. In terms of fuzzy sets, the created set will be different from classical set. Figure 5.1 draws attention to the degrees of membership to classical and fuzzy sets for this example.

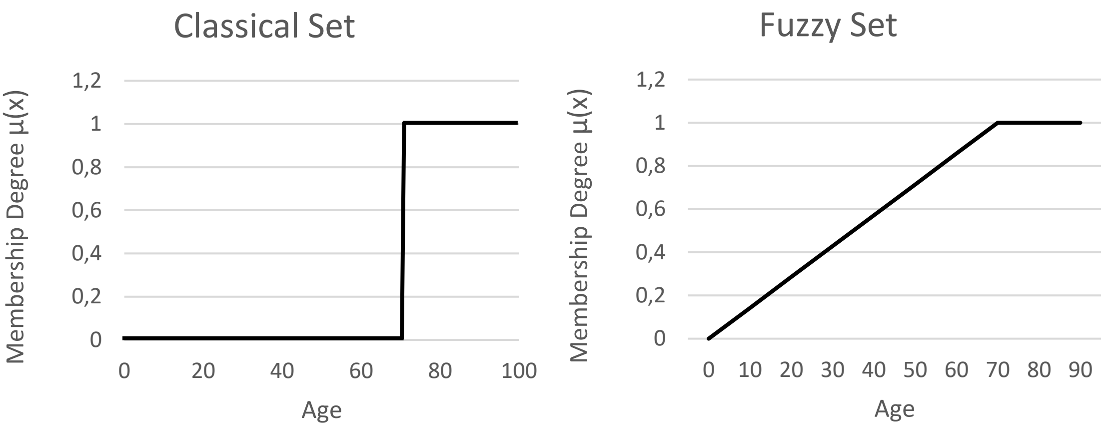

Figure 5.1 Classical Set and Fuzzy Set.

As seen above, a person's old age can be expressed in degrees in terms of membership degree. The belonging of an element to fuzzy sets is expressed by membership degrees and membership functions. The X-axis shows the set elements, the Y-axis shows the membership degrees of the elements in the set. A fuzzy set in X space formed by x elements can be expressed as follows.

$$A = \{(x, \mu_A(x)) | \ x \ \in X\} \tag{5.1}$$

There are no specific standard shapes for these functions. Shapes such as triangle, trapezoid, Gaussian, trapezoidal, Bell Curve, S, Z, Sigmoid, Cauchy can be used as membership functions. Among them, triangle, trapezoid and gaussian are the most used membership functions (Passino, Yurkovich, & Reinfrank, 1998). These functions are shown in Figure 5.2.

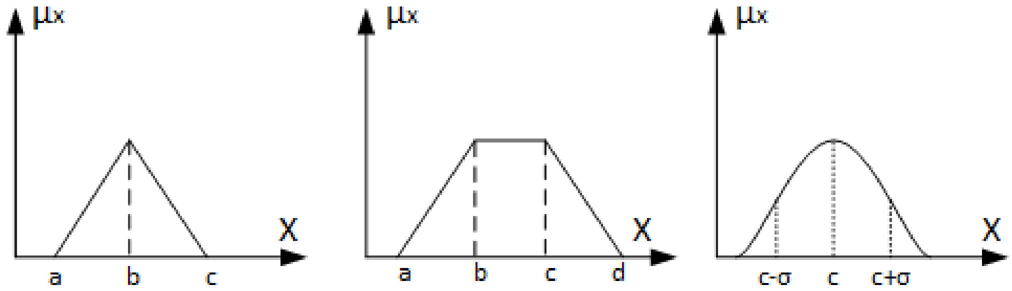

Figure 5.2. Triangular, Trapezoid, Gaussian Membership Functions.

All membership functions can be defined as $\mu_A(x)$: X → {0,1} which expresses boundary of membership degree of membership functions. Triangular membership function is defined in equation (5.2) below.

$$\mu(x; a, b, c) = \begin{cases} 0, & x < 0 \\ \frac{x-a}{b-a}, & a \leq x \leq b \\ \frac{c-x}{c-b}, & b \leq x \leq c \\ 0, & c < x \end{cases} \tag{5.2}$$

The mathematical expression of the trapezoidal membership function is in the equation (5.3).

$$\mu(x; a, b, c, d) = \begin{cases} 0, & x \leq a \\ \frac{x-a}{b-a}, & a \leq x \leq b \\ 1, & b \leq x \leq c \\ \frac{d-x}{d-c}, & c \leq x \leq d \\ 0, & d \leq x \end{cases} \tag{5.3}$$

Gaussian membership function is defined in equation (5.4).

$$\mu(x; c, \sigma) = e^{-\frac{1}{2}(\frac{x-c}{\sigma})^2} \tag{5.4}$$

5.2.2 Fuzzy Set Operations

Set operations are performed with fuzzy sets as in classical set theory. Zadeh made suggestions in his study for these fuzzy set operations (Lotti Zadeh, 1965).

Intersection, union and complementation operations are mostly used in applications. However, these operations are applied differently from classical set theory. As a representation, in fuzzy sets, the intersection of A and B sets is shown as A ∩ B, the union of sets A ∪ B and the complement of A set as $\bar{A}$. Accordingly, these operations can be expressed as seen in equations (5.5), (5.6) and (5.7).

$$A \cap B = \min \{ \mu_A(x), \mu_B(x) \} \tag{5.5}$$

$$A \cup B = \max \{ \mu_A(x), \mu_B(x) \} \tag{5.6}$$

$$\bar{A} = 1 - \mu_A(x) \tag{5.7}$$

The membership functions of the sets A and B are equal to the value of the membership function with the small one for intersection and the large one for union. Graphical representations of these operations are shown below.

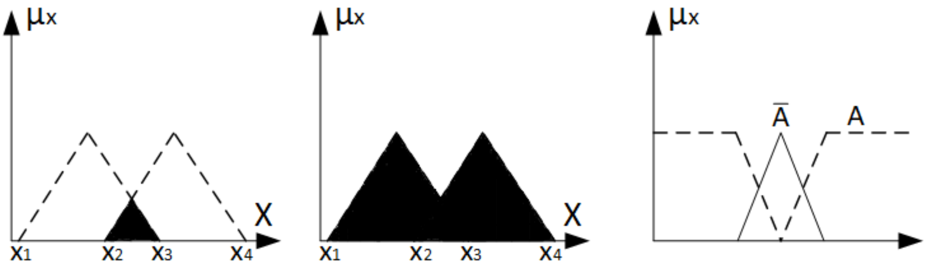

Figure 5.3. Intersection, Union and Complementation of Fuzzy Sets.

5.2.3 Fuzzy Inputs and Outputs

The properties of the physical system to be controlled are used as input variables in the fuzzy system. This input value or values are expressed by membership functions by performing the fuzzification process in the fuzzy logic system. Thus, the input values can be understood in terms of membership functions in the fuzzy system. After these values are evaluated in various ways in the fuzzy logic system, the outputs obtained are expressed in terms of output membership functions. Then, the output signals for the physical system are obtained by the defuzzification method.

5.2.4 Fuzzy Rules

In fuzzy logic controlled systems, fuzzy rules are created by making use of expert opinions and experiences. These rules are represented by the linguistic expressions IF-THEN. State (IF) and result (THEN) expressions here are expressed in terms of membership functions. For example, if IF Input is "Medium", THEN Output is imprecisely indicated as "Low" (Baykal & Beyan, 2004). According to this, if $X_1 = A_1$ and $X_2 = A_2$ ... $X_i = A_i$ then $Y_1 = B_1$ and $Y_2 = B_2$ and ... $Y_i = B_i$ can be represented as input and output fuzzy sets, respectively.

The number of fuzzy sets of the input variable determines the number of rules required. According to the designed system, the number of fuzzy sets for input or output variables can be up to 7. The required number of fuzzy rules should be written to accommodate the possible combinations of input variables. In some systems, dozens of rules can be created.

Considering an example multi-input single-output system, the list of rules can be created as follows in the light of the following assumptions (Pehlivan, 2001):

R_i = Fuzzy Logic Control Rule (i=1,2,3...n)

X,Y = Input State Variables

Z = Control Output Variable

A_i, B_i, C_i = Linguistic Values of X, Y, Z Variables.

$$R_1 = \text{IF } X = A_1 \text{ AND } Y = B_1 \text{ THEN } Z = C_1$$

$$R_1 = \text{IF } X = A_2 \text{ AND } Y = B_2 \text{ THEN } Z = C_2$$

...

$$R_n = \text{IF } X = A_n \text{ AND } Y_n = B_1 \text{ THEN } Z = C_n$$

In order to see these rules together, they are tabulated as follows.

Table 5.1 Fuzzy Rule Table.

X \ Y	B_1	B_2	B_3	B_4
A_1	C_1	...	...	...
A_2	...	C_2	...	...
A_3	...	...	...	...
A_4	...	...	...	...

5.3 Fuzzy Logic System

Fuzzy logic systems are systems that work using fuzzy set theory and IF-THEN rule structure. Fuzzy logic systems make matching between inputs and outputs with the help of fuzzy set theory. There are two types of fuzzy usage in fuzzy logic systems that emerged as a result of the studies of Mamdani and Sugeno (Mamdani, 1974; Takagi & Sugeno, 1985).

These two methods have similar and different aspects. In both Mamdani and Sugeno methods, the inputs are fuzzificated and applied to the system in this way. They differ in their output values. The linearity of the output membership functions and the expression of the outputs as functions of the input values differ in the Sugeno method.

Fuzzy logic systems created using one of these methods generally consist of fuzzification, rule base and inference mechanism and defuzzification parts. This structure is shown in Figure 5.4.

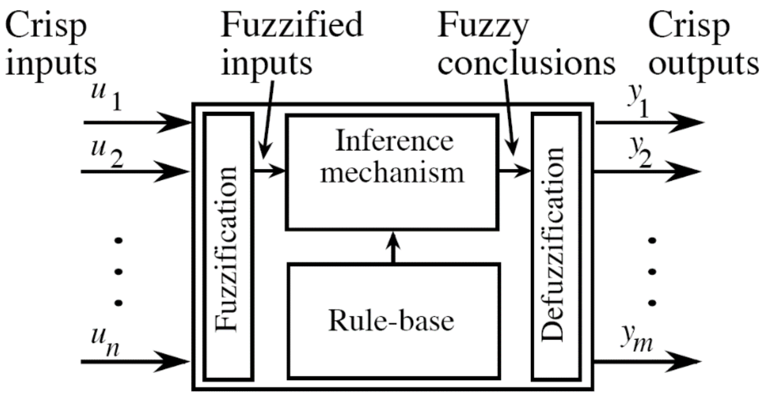

Figure 5.4. Fuzzy System (Passino et al., 1998)

The inputs of the fuzzy system are u_1, u_2, ... u_n, and the outputs are y_1, y_2, ... y_n. These input and output values are real number values. The fuzzification process transforms these values into fuzzy sets. Thanks to fuzzy rules, these sets are used to obtain fuzzy outputs and finally, fuzzy outputs are converted to crisp outputs with defuzzification process (Passino et al., 1998).

5.3.1 Fuzzification

Fuzzification is the process of converting crisp input values into fuzzy inputs. At the same time, the degree of membership of these values, which are expressed in terms of fuzzy inputs, to the appropriate fuzzy set is determined. These fuzzy inputs are then evaluated in the fuzzy inference mechanism using fuzzy rules.

Let U_i^* show all fuzzy sets that can be defined in U_i. By fuzzification the given u_i € U_i, it is transformed into a fuzzy set defined as $\hat{A}_i^{fuz}$ specified in the U_i universe of discourse. This operation is represented by the fuzzification operator F as follows:

$$F:\ U_i \rightarrow U_i^* \tag{5.8}$$

$$F(u_i) = \hat{A}_i^{fuz} \tag{5.9}$$

5.3.2 Rule Base and Inference Mechanism

The rule base is the structure of fuzzy rules created by considering all combinations with expert experience. The inference mechanism uses this rule base and creates a fuzzy set.

Mamdani and Sugeno type inference systems are generally used as inference mechanism. In the Mamdani type inference system, *the maximum of minimums (min-max)* and *maximum product (max-product) methods* are used.

In the maximum of minimums method, the membership degrees of these inputs in the input fuzzy set are determined separately for each rule, according to the crisp values of the inputs I_1 and I_2 at any moment. The minimum operator is applied to these membership degrees and a cropped fuzzy output set is obtained as much as the smallest membership degree obtained. This process is done for other rules as well, and fuzzy output is created as much as the number of rules. The maximum operator is applied to these, and a single fuzzy output set is obtained. Then, the crisp output value is calculated by defuzzification. This process is shown in Figure 5.5.

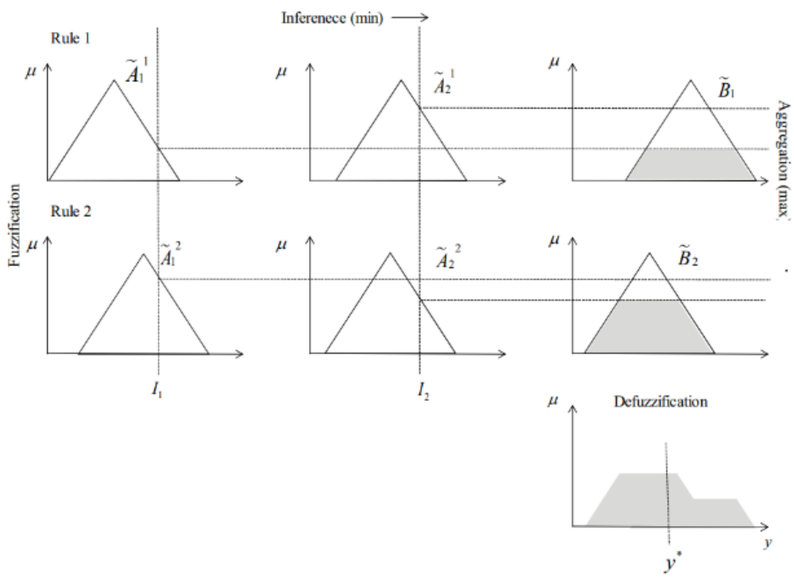

Figure 5.5. Mamdani Min-Max Method (Behret, UçaL, & Kahraman, 2012)

In the maximum-product method, the membership degrees of these inputs in the input fuzzy set are determined separately for each rule, according to the crisp values of the inputs I_1 and I_2 at any moment. These two crisp membership degrees are multiplied and the fuzzy output set determined at the smallest membership degree level is obtained. This process is done for other rules as well, and fuzzy output is created as much as the number of rules. These sets are unioned by applying the maximum operator. As a result, a fuzzy output set is obtained. Crisp output value is calculated by the defuzzification. This process is shown in Figure 5.6.

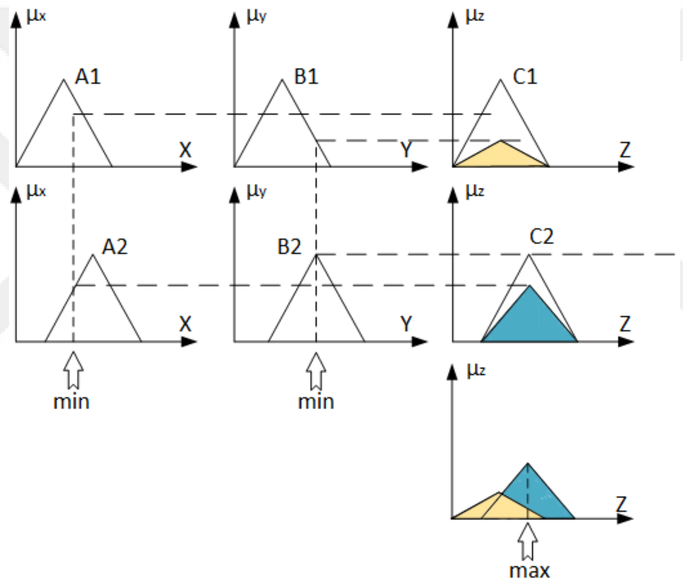

Figure 5.6. Mamdani Max-Product Method.

The fuzzy rule expressed in the Sugeno type inference system has the form "If X = A and Y = B then Z = $f(x,y)$ " (Takagi & Sugeno, 1985). Here, A and B fuzzy input sets are a function that gives fuzzy output dependent on x and y. The Sugeno type inference system expressed in this way is shown in Figure 5.7. Each rule has a crisp output value. The result is the weighted average of the outputs of each rule.

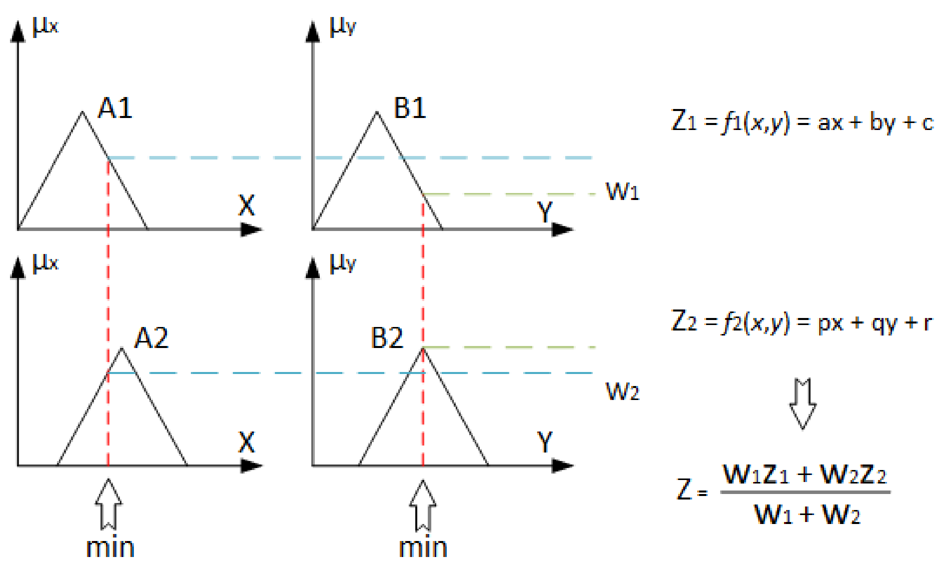

Figure 5.7. Sugeno Type Inference System.

5.3.3 Defuzzification

The outputs obtained with the fuzzy inference system are fuzzy values. By performing the defuzzification process, these fuzzy values are converted into real numerical values that can be applied to the external system. In the Defuzzification process, first the value consisting of membership degrees for the rules and the result rule are determined. Then the appropriate defuzzification method is selected and applied. The most used methods are:

- Center of gravity method
- Mean of maximums method
- Weighted average method
- Maximum membership method.

By applying the *center of gravity method* among these methods, the center of gravity of the shape formed by the fuzzy inference set is determined and this point is accepted as the output value. This method is expressed as:

$$z^* = \frac{\int \mu_c(z)\, z\, dz}{\int \mu_c(z)\, dz} \tag{5.10}$$

This method is visually expressed in Figure 5.8.

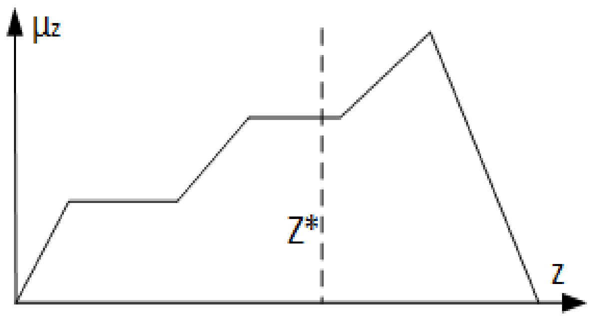

Figure 5.8 Center of Gravity Method.

Mean of maximums method can be preferred if there is more than one point with maximum membership degree. This method is mathematically represented by the equation below and it is expressed visually in the Figure 5.9.

$$z^* = \frac{a+b}{2} \tag{5.11}$$

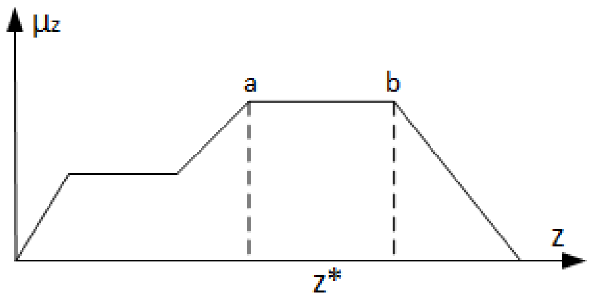

Figure 5.9 Mean of Maximums Method.

The weighted average method is one of the most commonly used methods. This method can be used when membership functions have symmetry. This method is mathematically represented by the equation below and it is expressed visually in the Figure 5.10.

$$z^* = \frac{\sum \mu_c(z)\, z}{\sum \mu_c(z)} \tag{5.12}$$

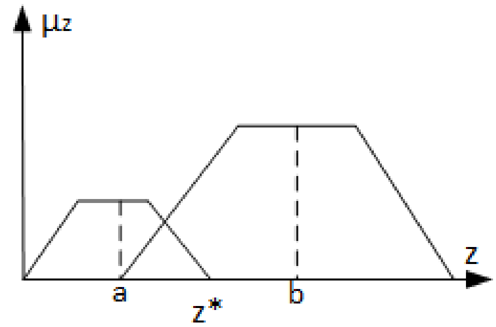

Figure 5.10 Weighted Average Method.

In order to use *the maximum membership method*, there must be a peak in the inference fuzzy set. The element with the highest value is used to get the output value. The operation of this algorithm becomes difficult when there is more than one maximum value. This method is mathematically represented by the equation below and it is expressed visually in the Figure 5.11.

$$\mu_c(z^*) \geq \mu_c(z),\ z \in Z \tag{5.13}$$

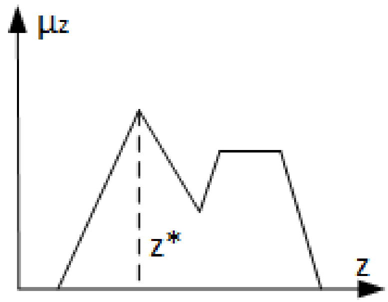

Figure 5.11 Maximum Membership Method.

5.4 Tuning of Fuzzy Logic Applications

Designing complex fuzzy logic applications is a challenging problem in terms of having a large number of input and output membership functions. In order to achieve the best results, while the fuzzy inference system is being designed, data-based approaches, manual approaches, learning fuzzy rules and tuning the parameters of the fuzzy inference system can be used. With these operations, the number of membership functions, their geometric shape and parameters, as well as fuzzy rules can be tuned. The more the number of variables to be tuned, the more time, process power and performance requirements will increase.

Tuning fuzzy inference systems is essentially an optimization problem. Many methods can be used to make this optimization. This process can be done manually or with the help of genetic, pattern search or other algorithms such as neural network, particle swarm optimization, Kalman filtering, gradient descent algorithms. In this section, only genetic algorithms and pattern search algorithms will be discussed briefly.

5.4.1 Tuning by Genetic Algorithms

Genetic algorithms are algorithms created by taking advantage of the working principles of biological evolution. These algorithms are algorithms that have been proven theoretically and practically to be resistant to working in complex environments and conditions (Goldberg & Holland, 1988).

Genetic algorithms are run with a population of randomly generated results. To improve the results, genetic processes are used with the help of genetic operators. These results enable the reproduction of results with better results with each generation through natural selection. An evaluation or fitness function distinguishes between good and bad results.

The advantage of genetic algorithms over other searching algorithms is that they do not need gradient information or continuity assumption when searching for the best parameters. They can investigate many characteristics at once, as would be required when dealing with complex problems (Dao & Chen, 2012).

5.4.2 Tuning by Pattern Search Algorithms

The pattern search method consists of a pattern in a geometric pattern and a step length value around a starting point. Extremity points equidistant from the starting point will be the center of the pattern. At these extremity points of the pattern, the best point among the values tested with the objective function will be the center point of the new pattern, and the pattern search method will be reproduced in a way that will move towards the optimum point. When a better test result cannot be obtained at the extremity points, the pattern will be shrinked by reducing the step length. The search will stop when the step length falls below a specific tolerance. For instance, with the pattern search method membership functions can be tuned in this study (Tremante, Yen, & Brea, 2019).

5.5 Sensing Principle of Developed Sensor and Applied Algorithm

The developed spherical sensor is worked by evaluating the data received from the light sensors placed on it. This evaluation is made within the scope of an algorithm in which fuzzy logic is also used.

Test data is first acquired with the help of the TSA method mentioned in Chapter 4. Thus, high frequency and noise components are filtered out in the measured data. In the next step, the mean of significant values (0 lux or lux values not very close to 0) among the measured values is classified according to the illumination values in the $I(\bar{x})$ function.

$$I(\bar{x}) = \begin{cases} Weak\ Light\ Source, 0 < \bar{x} < 500\ lux \\ Medium\ Level\ Light\ Source, 500 < \bar{x} < 1000\ lux \\ High\ Level\ Light\ Source, \bar{x} > 1000\ lux \end{cases} \tag{5.14}$$

According to this classification, the fuzzy set's parameters are tuned and arranged in the fuzzification phase of fuzzy logic application. This part will be explained in detail in the continuation of the study. The diagram below shows the sensing principle of the developed sensor and the general operation of the algorithm used.

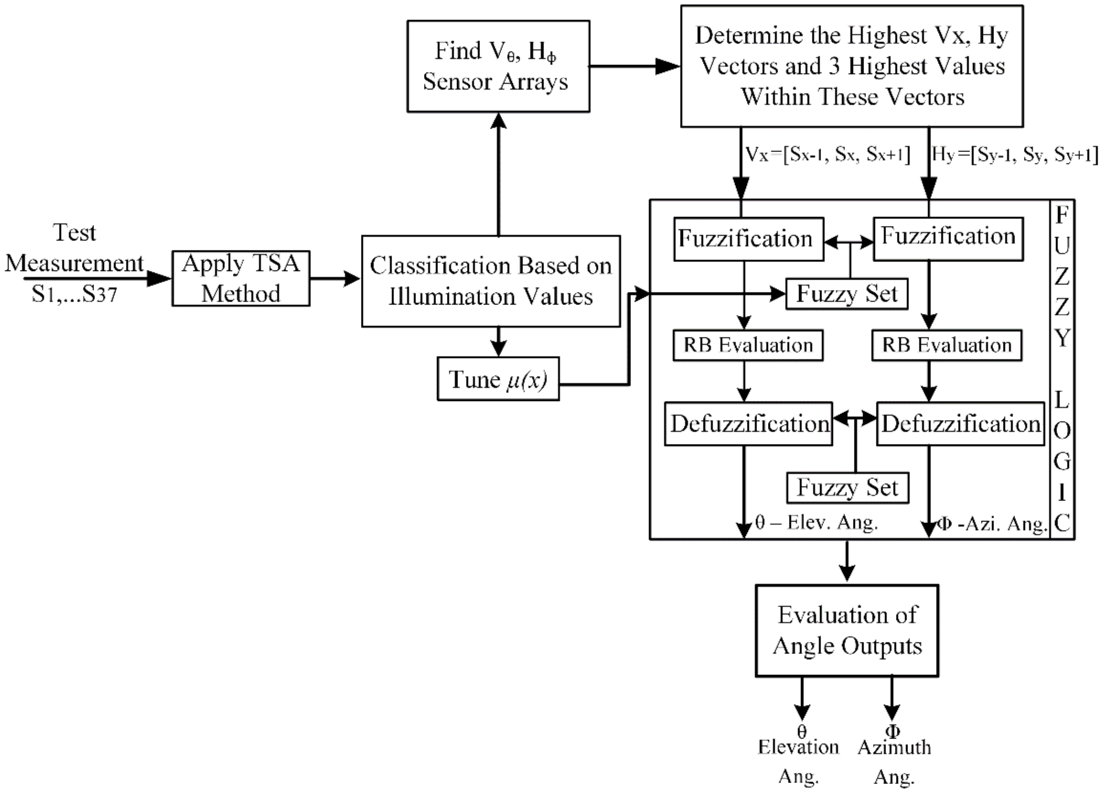

Figure 5.12 Sensing Principle and Applied Fuzzy Logic Algorithm.

V_θ and H_Φ sensor arrays were created by utilizing the measurement data classified as weak, medium or high level light source. Among these series, V_θ arrays are vertical arrays and represent the sensor arrays formed in the direction of elevation angle. H_Φ arrays, on the other hand, are horizontal arrays and represent the sensor arrays formed in the azimuth direction.

Sensor points in the spherical coordinate plane are expressed as $P(r, \theta, \varphi)$. The sensors placed at the intervals θ elevation angle, $\theta = [0, \pi/2]$ and φ azimuth angle, $\varphi = [0.2\pi]$ in the spherical plane are numbered as $S_1, S_2, S_3 \ldots S_{37}$. The sensors compose arrays of sensors vertically in the direction of the angle θ, denoted by,

$$V_\theta = \begin{pmatrix} V_1 \\ V_2 \\ \vdots \\ V_{12} \end{pmatrix} \tag{5.15}$$

$$\left.\begin{aligned} V_1 &= (S_1, S_2, S_3, S_{37}) \\ V_2 &= (S_4, S_5, S_6, S_{37}) \\ &\dots \end{aligned}\right\} \tag{5.16}$$

The sensors compose arrays of sensors horizontally in the direction of the angle φ, denoted by,

$$H_\varphi = \begin{pmatrix} H_1 \\ H_2 \\ H_3 \\ H_4 \end{pmatrix} \tag{5.17}$$

$$\left.\begin{aligned} H_1 &= (S_1, S_4, S_7, S_{10}, S_{13}, S_{16}, S_{19}, S_{22}, S_{25}, S_{28}, S_{31}, S_{34}) \\ H_2 &= (S_2, S_5, S_8, S_{11}, S_{14}, S_{17}, S_{20}, S_{23}, S_{26}, S_{29}, S_{32}, S_{35}) \\ H_3 &= (S_3, S_6, S_9, S_{12}, S_{15}, S_{18}, S_{21}, S_{24}, S_{27}, S_{30}, S_{32}, S_{36}) \\ H_4 &= (S_{37}) \end{aligned}\right\} \tag{5.18}$$

The V_θ and H_φ sensor arrays are shown in Figure 5.13 and Figure 5.14.

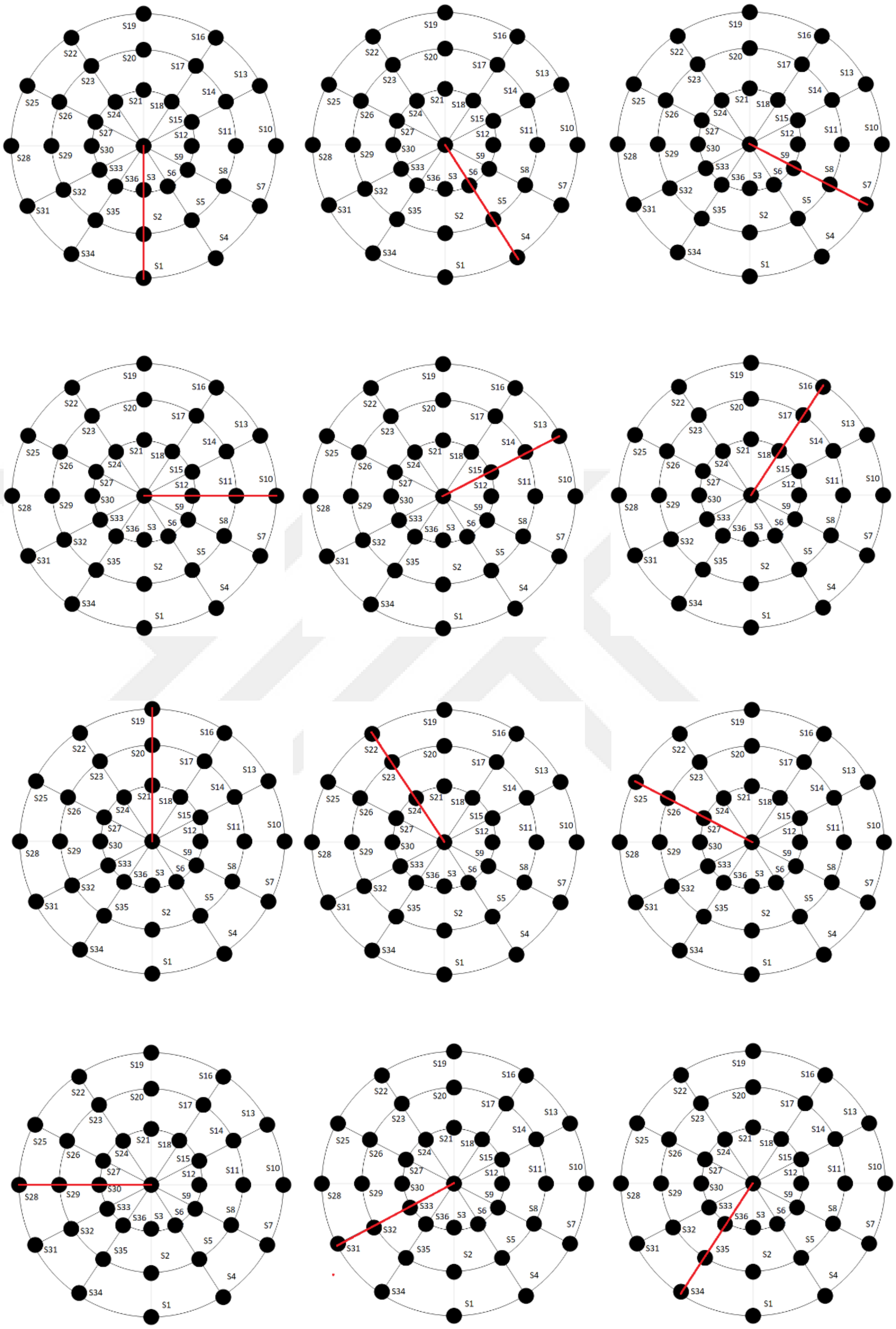

Figure 5.13. V_θ sensor arrays.

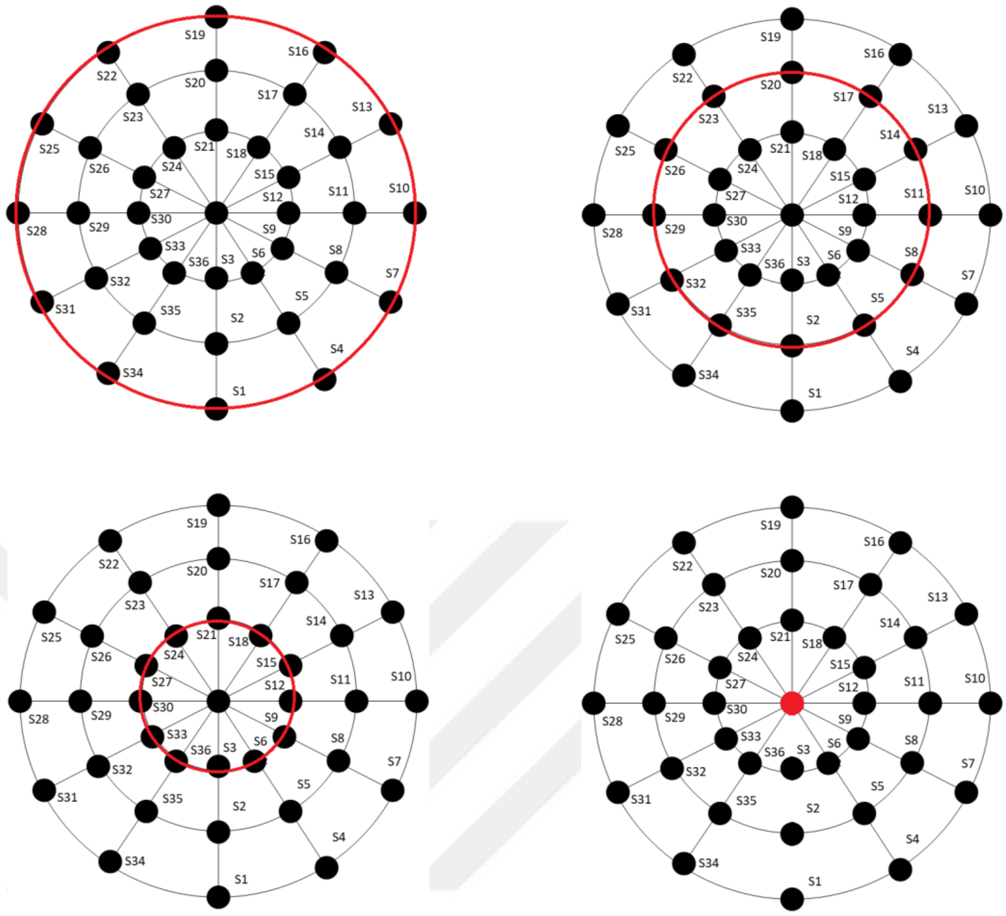

Figure 5.14. H_{φ} sensor arrays.

The composed V_{θ} and H_{φ}sensor arrays are scanned in groups and the highest value sensors are detected. The sensor group in which the 3 sensors with the highest value are together is determined. This is done for all sensor arrays in V_{θ} and H_{φ}. Finally, 3 array elements are determined to be used as inputs in fuzzy logic application. These sensor arrays are called V_x and H_y, and the sensors they house are shown in the figure below.

$$V_x = [S_{x-1}, S_x, S_{x+1}] \qquad H_y = [S_{y-1}, S_y, S_{y+1}] \qquad (5.19)$$

5.6. Determined Fuzzy Basics on Developed Sensor

The V_x and H_y sensor arrays obtained from the data measured on the developed sensor are used as input variables in the fuzzy logic application. In the study, two different fuzzy models were used to determine the elevation and azimuth angles.

In the software where V_x and H_y sensor arrays are used, the S_x and S_y sensor values in the center of the arrays always consist of the highest value sensors. This sorting has provided an advantage both in obtaining the angular outputs and in the creation of the fuzzy rule base. Thus, a significant reduction in the number of defined fuzzy rules has been achieved. These variables, which are used as fuzzy inputs, can be seen in Figure 5.15.

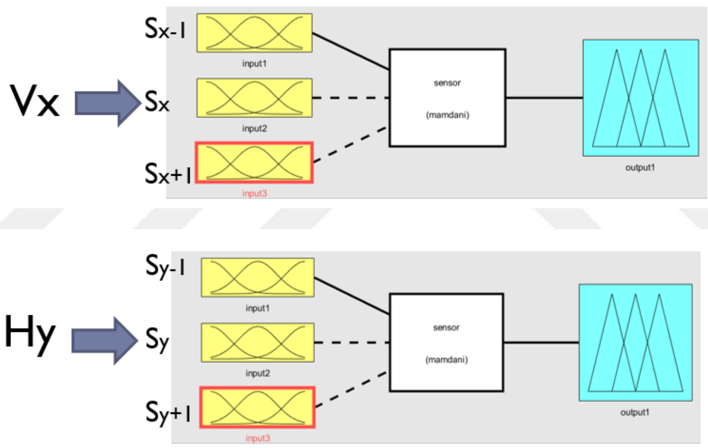

Figure 5.15 Input variables for Elevation and Azimuth Angles.

In response to these input variables, output angle values in the range of $[0, \pi/3]$ are obtained for both angles at the output of the fuzzy logic application. However, these values are not the final values obtained for the output angles. In the rest of the software (Evaluation of Angle Outputs Section), these angles are regulated by determining the input variables for the sensor arrays. Namely, with the determination of the input variables, the azimuth and elevation angles, where the light source is measured most intensely, are offset, especially thanks to the knowledge of the sensors located in the center. The output angle values obtained are regulated by this information.

Input variables are expressed in terms of membership functions in the fuzzification section. Input membership functions are shown in Figure 5.16.

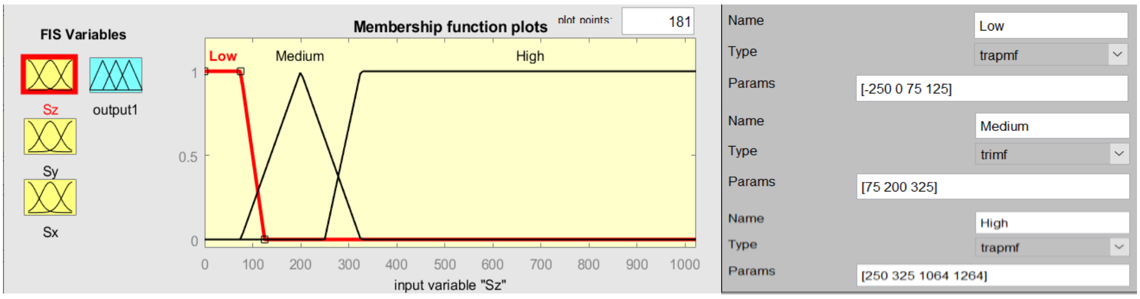

Figure 5.16 Membership Functions of Input Variables.

When examined with expert knowledge, Low membership function was determined in trapezoid form with parameters [-250 0 75 125] according to enviroment conditions and test light source data. Medium membership function in triangular form [75 200 325] and High membership function are determined by [250 325 1064 1264] parameters. Output variables and membership functions are shown in Figure 5.17.

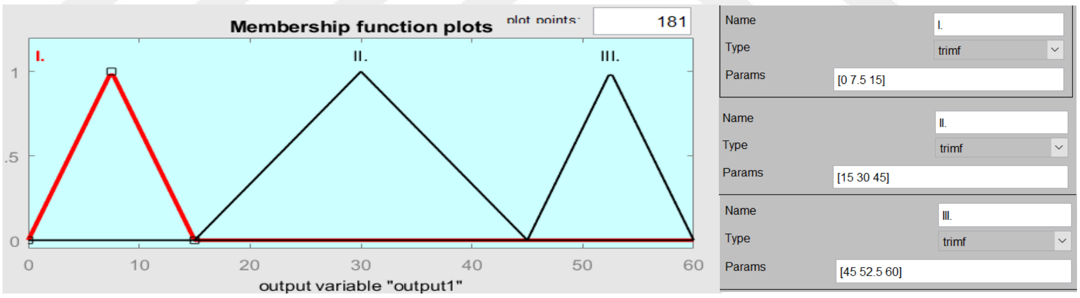

Figure 5.17 Membership Functions of Output Variables.

Regions I, II and III are defined for the output membership functions. Outputs from these regions were evaluated in the next step.

The rule base was used in the fuzzy inference part of the created fuzzy block. As stated before, the number of fuzzy rules to be created is significantly reduced thanks to the sequence of input variables. However, 42 rules were created. A few of these rules are shown below:

- If (Sz is Low) and (Sy is Low) and (Sx is Low) Then (Output1 is II).
- If (Sz is Low) and (Sy is Medium) and (Sx is Low) Then (Output1 is II).
- If (Sz is Medium) and (Sy is Medium) and (Sx is Medium) Then (Output1 is II).
- If (Sz is Low) and (Sy is High) and (Sx is Low) Then (Output1 is II).
- If (Sz is Medium) and (Sy is High) and (Sx is Medium) Then (Output1 is II).
- If (Sz is High) and (Sy is High) and (Sx is High) Then (Output1 is II).
- If (Sz is Medium) and (Sy is Medium) and (Sx is Low) Then (Output1 is II).
- If (Sz is High) and (Sy is High) and (Sx is Low) Then (Output1 is III).
- If (Sz is Low) and (Sy is High) and (Sx is High) Then (Output1 is I).
- If (Sz is High) and (Sy is High) and (Sx is Medium) Then (Output1 is III).

The output values obtained were converted to real values by using the *center of gravity method* in the defuzzification section.

CHAPTER SIX

RESULTS AND CONCLUSION

6.1 Results

6.1.1 Visual Outputs of Collected Data

In the study, numerical sensor data were obtained to ensure the localization of the light source. In addition, spherical representations were made in order to interpret the location of the light source by using these numerical data.

In the experimental measurements, the distance between the light source and the developed sensor was kept constant except one measurement. In addition, the position of the light source was changed in the direction of azimuth and elevation angles, and the data were recorded in this way. Table 6.1 shows the data for the measurements made.

Table 6.1 Measurement Data.

Measurement Number	d (cm)	R (cm)	h (cm)	Corresponded Reference Sensor	Elevation Angle (θ)	Azimuth Angle (ϕ)
1	40	40	0	S1	0	0
2	40	46.19	23.09	S2	30	0
3	40	80	69.28	S3	60	0
4	40	-	-	S37	90	-
5	80	-	-	S37	90	-

Figure 6.1 and Figure 6.2 represent the polar and spherical representations formed as a result of the measurements. In the measurements seen in Figure 6.1, the azimuth angle was kept constant and the elevation angle was changed. It is seen that there is a difference between the measurements in terms of the illumination values. Values measured in M1 are 0 – 400 Lux, values measured in M2 are 0 – 250 Lux, values measured in M3 are in the range of approximately 0 – 40 lux. In these 3 measurements,

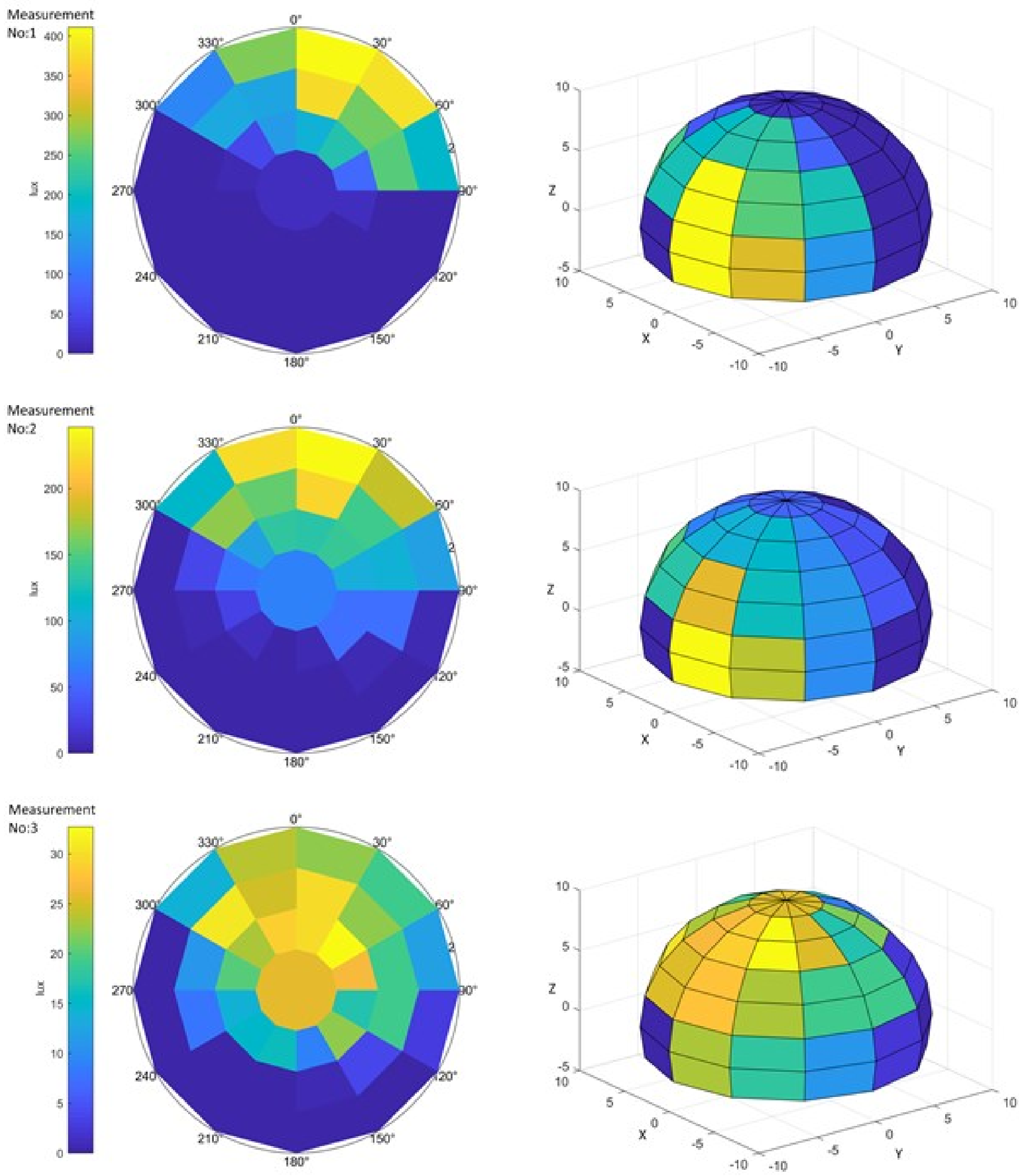

Figure 6.1 Polar Coordinates and Spherical Representation of M1-M2-M3 Measurements.

the position of the light source was increased in the direction of elevation angle. Thus, it is seen that the light beams scatter more and the measured values decrease.

In Figure 6.2, measurements were made from different distances with the light source pointed at the S37 sensor located at the apex of the sphere. A similar situation can be seen here in terms of the intensity of illumination between the measurements.

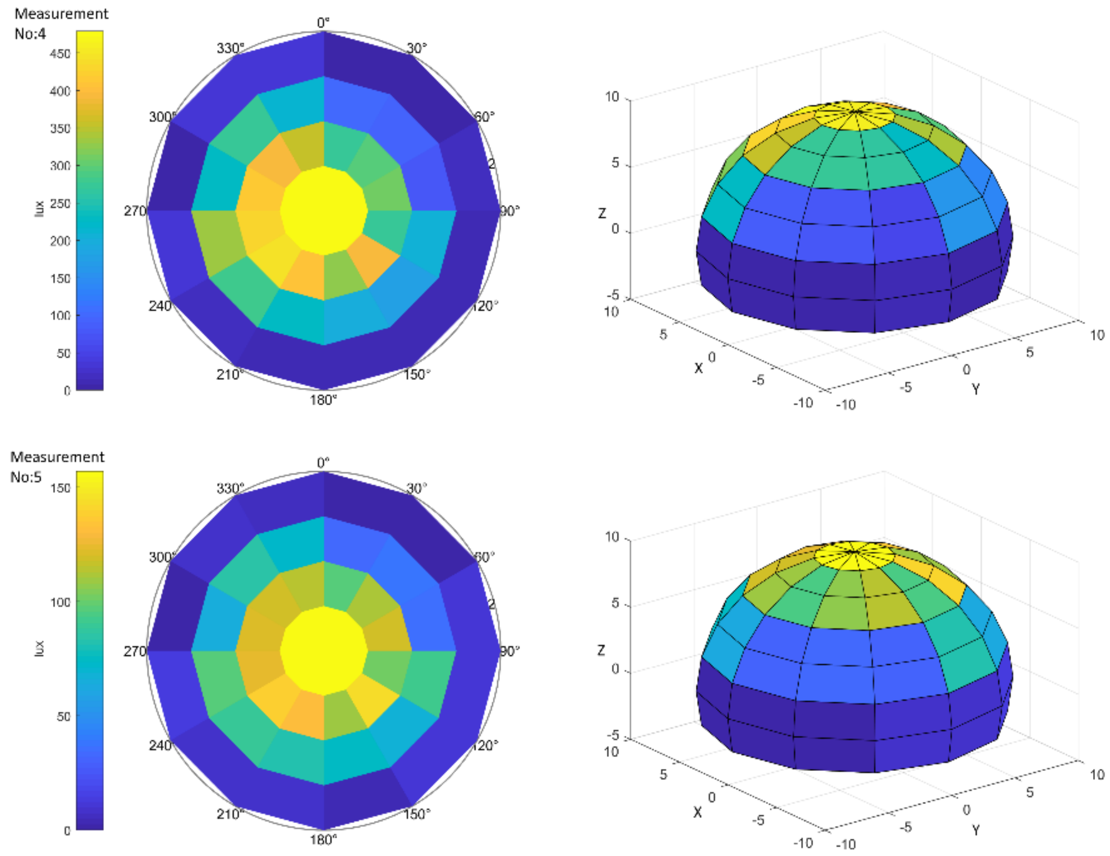

Figure 6.2 Polar Coordinates and Spherical Representation of M4-M5 Measurements.

While values in the range of 0-450 lux were recorded in the measurement of d=40 cm, values in the range of 0-150 lux were recorded in the measurement of d=80 cm. However, it is seen that the distribution has the highest value in both measurements in the S37 sensor located in the center and gradually decreases with decreasing elevation angles.

Visual test results represented in polar and spherical coordinates are numerically expressed in Table 6.2.

Table 6.2 Measurement Results.

MEASUREMENT VALUES				MEASURED OUTPUTS	
Measurement Number	Corresponded Reference Sensor	Elevation Angle (θ)	Azimuth Angle (ϕ)	Elevation Angle (θ)	Azimuth Angle (ϕ)
1	S1	0	0	4,7	2,3
2	S2	30	0	27,1	2,8
3	S3	60	0	57,8	3,4
4	S37	90	-	85,3	-
5	S37	90	-	84,8	-

The experimental measurement values in the table are compared with the numerical outputs. It is seen that the numerical results represent similar results with the experimental measurement values and visual outputs.

6.1.2 Numerical Results of Collected Solar Data

In this part of the study, the results obtained by operating the developed spherical sensor in outdoor conditions are presented. Experimental data were collected on a clear sky day. The spherical sensor is oriented to the north with the help of a digital compass. The sensors S1, S2, S3, located in the azimuth 0 ° position of the spherical sensor, are positioned so that they are geographically equal to the north direction. Its positioning in terms of elevation angle was carried out empirically in such a way as to prevent the interference of elevations or obstacles. These adjustments are important for solar calculations. As in the studies conducted in the literature, positioning can be done more precisely by using barometric and astronomical data. Accordingly, information about the measurements is shown in Table 6.3.

Table 6.3 Information about the measurements.

Date	18.03.2022
Time	10:00 – 11:00
Weather Condition	Clear Sky
Location	Bornova, İzmir, Turkey
Time Zone	UTC (+03:00)
Coordinates	38° 28' 15.7"N, 27° 14' 54.7"E

The measurements taken according to the information in Table 6.3 were recorded and the calculated solar elevation and azimuth angles were obtained using the solar angular equations (2.4), (2.6) and (2.7). Accordingly, some measurement results obtained in the specified time interval and their comparison with calculated solar angles are shown in Table 6.4.

Table 6.4 Sample Results and Comparison.

Time	Calculated Elevation Ang. (θ)	Calculated Azimuth Ang.(ϕ)	Measured Elevation Ang.(θ)	Measured Azimuth Ang.(ϕ)
10:00	29,60°	118,56°	32,23°	125,17°
10:15	32,14°	121,78°	34,58°	127,87°
10:30	34,59°	125,18°	37,31°	129,64°
10:45	36,93°	128,78°	39,94°	135,96°
11:00	39,16°	132,62°	41,64°	141,37°

Measurements made in the specified time interval were examined. Elevation angle, azimuth angle and error values for these measured values are shown in Figure 6.3 and Figure 6.4.

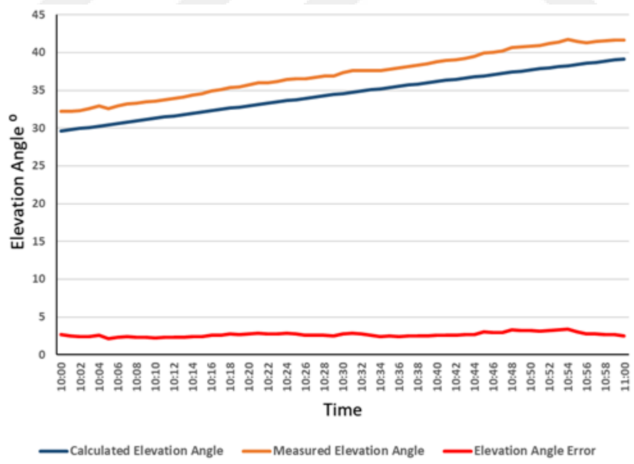

Figure 6.3 Calculated, Measured Elevation Angles and Error.

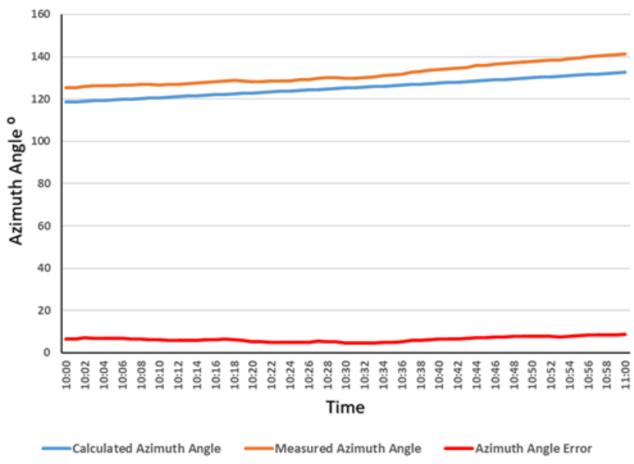

Figure 6.4 Calculated, Measured Azimuth Angles and Error.

By examining the measured values, the error metric values obtained from these values are shown in Table 6.5. MAD (Mean Absolute Deviation), MSE (Mean Square Error), RMSE (Root Mean Square Error) and MAPE (Mean Absolute Percentage Error) metrics were used in the preparation of the table.

Table 6.5 Error Metrics of Measured Values.

	MAD	MSE	RMSE	MAPE
Azimuth Angle Error	6,41	42,52	6,52	5,10
Elevation Angle Error	2,66	7,16	2,67	7,71

The outputs of the measurements obtained and the metrics created based on these outputs were evaluated. Although there are error values determined in azimuth and elevation angles, the outputs obtained will give functional results in practical applications. However, considering the studies in the literature, it is necessary to make improvements especially in the mean absolute percentage error rates (see MAPE).

Errors in question may be the results of fuzzy blocks which are used in control algorithm. It may be necessary to review the fuzzy rules based on expert opinion and experience and make additions in order to minimize error values.

It is observed that the measured error values also differ in terms of azimuth and elevation angles. This difference in the outputs should also be taken into account during the review.

6.2 Conclusions

This work focuses on designing a spherical solar sensor with high accuracy that can be used in solar tracking systems. For this purpose, a novel designed sensor solid model was used. This model is supported by light sensors and electronic circuits. Fuzzy logic is used to localize the light source with the help of data from light sensors.

There are many studies on solar tracking systems and sun sensors in the literature. These studies focused on various problems of solar energy systems. Collecting the highest energy from the sun is one of these problems. In order to do this, the position of the sun in the sky must be determined accurately.

Many methods have been proposed that provide a solution to this issue. LDRs have been a frequently used circuit element, especially in the first period studies. LDRs are preferred because they are cheap, easily available and useful. In addition, it is not possible to establish high-accuracy systems using LDRs. Systems that use geographic location and time-date information also achieve good results. In these systems, there is a need to make astronomical calculations or to provide these data from external sources. Obtaining these data by calculating instantaneously brings with it high computational needs in the area where these systems are located. With the development of sensor technologies, technologies such as MEMS, in which microelectronic circuits are used, have also contributed to the field of solar energy. These technologies have provided high accuracy data to be obtained. In addition, the difficulty of production and high cost prevent their widespread use. Image processing technologies have also become one of the solutions that require intensive computation in order to establish high-accuracy systems in this field.

When all the proposed methods are examined, it is seen that each of them has advantages and disadvantages. In this context, it is seen that there is a need for cost-effective and highly accurate solutions. In addition, it stands out as the desired features that these solutions do not require intensive calculations and geographical information.

In this thesis work, we aimed to contribute to filling this gap in the literature. Our aim was to find a solution for the localization of the sun in the sky. For this purpose, studies were carried out on two subjects; i) design a novel spherical sensor that will collect data on the location of the light source, and ii) obtain a compact structure that will enable the localization of the light source with the help of the fuzzy logic model used in this designed sensor. In the first part of the study, a 3D sphere model was created to take advantage of spherical data collection. In order to obtain the data, appropriate light sensors were determined and studies were carried out to realize the optimum use in this design. In this context, it was determined that the most appropriate sensor angular interval should be 30° for a sphere with the determined diameter. Accordingly the sensors are placed in the spherical model. In this section, electronic circuits that transmit the data measured by the sensor to the computer environment are designed. The data from the sensors were taken by the TSA method and thus cleared of various noises and high frequency components. The designed measurement system is optimized in terms of speed and accuracy. In the second part of the study, a software has been developed in which fuzzy logic model is also used. The algorithm used tunes the membership functions in the fuzzy model in accordance with the different conditions of light intensity.

In the study, numerical angle outputs and visual results related to the localization of the light source were obtained. The final system has a resolution depending on the number of sensors used. This resolution is at a level that can accurately localize the source in solar energy applications. However, considering the different usage areas of the sensor - for example in robotics - it may be necessary to adapt the number of sensors. This will cause an increase in the complexity of the system.

6.3 Future Works

This study can inspire future academic or industrial studies. Some of the possible future works are listed below.

- This study can be made more compact and standalone and can be turned into a sensor that can be used directly at the point where it is positioned with appropriate processing capacity and can be directly integrated into solar tracking systems. In order to implement this improvement, studies can be made by using embedded systems.

- The studies that can be done on the production technology of the sensor solid model can be transformed into a solid model where more sensors can be used together and can be optimized in terms of sensor placements.

- The spherical sensor structure will be able to find new areas of use in indoor environments with light sensors that will operate at different wavelengths. For example, it can be used for location coordination of mobile robots working in dark factories.

- Neural network or deep learning algorithms can be used to increase the performance of the sensor in the localization process. Angular outputs to be obtained in the experimental environment with light sensors will provide datasets that can be used efficiently in neural network applications. Thus, meaningful results can be obtained about the angular outputs and the position of the light source.

REFERENCES

Abdallah, S., & Nijmeh, S. (2004a). Two axes sun tracking system with PLC control. *Energy Conversion and Management*, *45*(11–12), 1931–1939. https://doi.org/10.1016/j.enconman.2003.10.007

Abdollahpour, M., Golzarian, M. R., Rohani, A., & Abootorabi Zarchi, H. (2018). Development of a machine vision dual-axis solar tracking system. *Solar Energy*, *169*(February), 136–143. https://doi.org/10.1016/j.solener.2018.03.059

Ajay, K., & Nagaraju, J. (2003). Micro-controller based sun tracker for line focus concentrating collectors. *SESI Journal: Journal of the Solar Energy Society of India*, *13*(1/2), 1.

Ak, N., & Demirbas, A. (2016). Promising sources of energy in the near future. *Energy Sources, Part A: Recovery, Utilization, and Environmental Effects*, *38*(12), 1730–1738.

Al-mohamad, A. (2004). Applied Efficiency improvements of photo-voltaic panels using a Sun-tracking system, *79*, 345–354. https://doi.org/10.1016/j.apenergy.2003.12.004

Al-Naima, F. M., & Yaghobian, N. A. (1990). Design and construction of a solar tracking system. *Solar & Wind Technology*, *7*(5), 611–617. https://doi.org/https://doi.org/10.1016/0741-983X(90)90072-A

Alata, M., Al-Nimr, M. A., & Qaroush, Y. (2005). Developing a multipurpose sun tracking system using fuzzy control. *Energy Conversion and Management*, *46*(7), 1229–1245. https://doi.org/https://doi.org/10.1016/j.enconman.2004.06.013

Alorda, B., Pujol-Nadal, R., Rodriguez-Navas, G., Moià-Pol, A., & Martínez-Moll,

V. (2015). Collaborative distributed sun-tracking control system for building integration with minimal plant area and maximum energy-conversion efficiency. *International Journal of Electrical Power & Energy Systems*, *70*, 52–60. https://doi.org/https://doi.org/10.1016/j.ijepes.2015.01.038

Anderson, E., Dohan, C., Sikora, A., Bitar, S. J., & McNeill, J. A. (2003). Solar panel peak power tracking system. *Worcester Polytechnic Institute*, *12*, 28–30.

Anderson, J. A., Silverstein, J. W., Ritz, S. A., & Jones, R. S. (1977). Distinctive features, categorical perception, and probability learning: Some applications of a neural model. *Psychological Review*, *84*(5), 413–451. https://doi.org/10.1037/0033-295X.84.5.413

Barlev, D., Vidu, R., & Stroeve, P. (2011). Innovation in concentrated solar power. *Solar Energy Materials and Solar Cells*, *95*(10), 2703–2725. https://doi.org/10.1016/j.solmat.2011.05.020

Baykal, N., & Beyan, T. (2004). *Bulanık mantık: uzman sistemler ve denetleyiciler*. Bıçaklar Kitabevi.

Behret, H., Uçal, İ., & Kahraman, C. (2012). Multicriteria Evaluation of Environmentally Conscious Manufacturers Under Fuzzy Environment. *Journal of Multiple-Valued Logic & Soft Computing*, *18(6)*, 467.

Bhatia, S. C. (2014). 2 - Solar radiations. In S. C. B. T.-A. R. E. S. Bhatia (Ed.) (pp. 32–67). Woodhead Publishing India. https://doi.org/https://doi.org/10.1016/B978-1-78242-269-3.50002-4

Birol, F. (2006). World energy prospects and challenges. In *CESifo Forum* (Vol. 7, pp. 3–7). München: ifo Institut für Wirtschaftsforschung an der Universität München.

Blanco-Muriel, M., Alarcón-Padilla, D. C., López-Moratalla, T., & Lara-Coira, M. (2001). Computing the solar vector. *Solar Energy*, *70*(5), 431–441. https://doi.org/https://doi.org/10.1016/S0038-092X(00)00156-0

Carballo, J. A., Bonilla, J., Berenguel, M., Fernández-Reche, J., & García, G. (2019). New approach for solar tracking systems based on computer vision, low cost hardware and deep learning. *Renewable Energy*. https://doi.org/10.1016/j.renene.2018.08.101

Chen, F., Feng, J., & Hong, Z. (2006). Digital sun sensor based on the optical vernier measuring principle. *Measurement Science and Technology*, *17*(9), 2494–2498. https://doi.org/10.1088/0957-0233/17/9/017

Chong, K. K., & Wong, C. W. (2009). General formula for on-axis sun-tracking system and its application in improving tracking accuracy of solar collector. *Solar Energy*, *83*(3), 298–305. https://doi.org/https://doi.org/10.1016/j.solener.2008.08.003

Clifford, M. J., & Eastwood, D. (2004). Design of a novel passive solar tracker. *Solar Energy*, *77*(3), 269–280.

da Rocha Queiroz, J., da Silva Souza, A., Gussoli, M. K., de Oliveira, J. C., & Andrade, C. M. (2020). Construction and Automation of a Microcontrolled Solar Tracker. *Processes* . https://doi.org/10.3390/pr8101309

Dao, T.-K., & Chen, C.-K. (2012). Tuning fuzzy-logic controllers. In *Fuzzy Logic-Controls, Concepts, Theories and Applications* (pp. 351–372). InTech.

Darula, S., Kittler, R., & Gueymard, C. A. (2005). Reference luminous solar constant and solar luminance for illuminance calculations. *Solar Energy*, *79*(5), 559–565.

Davies, P. A. (1993). Sun-tracking mechanism using equatorial and ecliptic axes.

Solar Energy, *50*(6), 487–489. https://doi.org/https://doi.org/10.1016/0038-092X(93)90110-A

Delgado, F. J., Quero, J. M., Garcia, J., Tarrida, C. L., Ortega, P. R., & Bermejo, S. (2012). Accurate and Wide-Field-of-View MEMS-Based Sun Sensor for Industrial Applications. *IEEE Transactions on Industrial Electronics*, *59*(12), 4871–4880. https://doi.org/10.1109/TIE.2012.2188872

Dezfooli, A. S., Nejad, F. M., Zakeri, H., & Kazemifard, S. (2017). Solar pavement: A new emerging technology. *Solar Energy*, *149*, 272–284. https://doi.org/https://doi.org/10.1016/j.solener.2017.04.016

Dijkshoorn, A., Werkman, P., Welleweerd, M., Wolterink, G., Eijking, B., Delamare, J., … Krijnen, G. J. M. (2018). Embedded sensing: Integrating sensors in 3-D printed structures. *Journal of Sensors and Sensor Systems*, *7*(1), 169–181. https://doi.org/10.5194/jsss-7-169-2018

Drummond, A. J., Hickey, J. R., Scholes, W. J., & Laue, E. G. (1968). New value for the solar constant of radiation. *Nature*, *218*(5138), 259–261.

Edwards, B. P. (1978). Computer based sun following system. *Solar Energy*, *21*(6), 491–496. https://doi.org/https://doi.org/10.1016/0038-092X(78)90073-7

Elmaged, A., & Kamal, H. (2015). *Passive solar tracking system.* Doctoral dissertation, University of Khartoum, Sudan.

Eubanks, T. M. (1993, January 1). Variations in the Orientation of the Earth. *Contributions of Space Geodesy to Geodynamics: Earth Dynamics*. https://doi.org/https://doi.org/10.1029/GD024p0001

Finster, C. (1962). El heliostato de la Universidad santa maria. *Scientia*, *119*, 5–20.

Garcia-Gil, G., & Ramirez, J. M. (2019). Fish-eye camera and image processing for commanding a solar tracker. *Heliyon*, *5*(3), e01398. https://doi.org/10.1016/j.heliyon.2019.e01398

Garrido, R., & Díaz, A. (2016). Cascade closed-loop control of solar trackers applied to HCPV systems. *Renewable Energy*, *97*, 689–696. https://doi.org/https://doi.org/10.1016/j.renene.2016.06.022

Gay, C. F., Yerkes, J. W., & Wilson, J. H. (1982). Performance advantages of two-axis tracking for large flat-plate photovoltaic energy systems. In *16th Photovoltaic Specialists Conference* (pp. 1368–1371).

Gevorkian, P. (2010). *Alternative energy systems in building design*. McGraw-Hill Education.

Goldberg, D. E., & Holland, J. H. (1988). Genetic algorithms and machine learning. *Machine Learning*, *3*(2), 95-99.

Gräbner, D., Dödtmann, S., Dumstorff, G., & Lucklum, F. (2018). 3-D-printed smart screw: Functionalization during additive fabrication. *Journal of Sensors and Sensor Systems*, *7*(1), 143–151. https://doi.org/10.5194/jsss-7-143-2018

Grena, R. (2008). An algorithm for the computation of the solar position. *Solar Energy*, *82*(5), 462–470. https://doi.org/https://doi.org/10.1016/j.solener.2007.10.001

Hamilton, J. D. (2009). Understanding crude oil prices. *The Energy Journal*, *30*(2), 35.

Hızarcı, B., Ümütlü, R. C., Kıral, Z., & Öztürk, H. (2021). Fault severity detection of a worm gearbox based on several feature extraction methods through a developed condition monitoring system. *SN Applied Sciences*, *3*(1), 129.

https://doi.org/10.1007/s42452-020-04131-w

Hottel, H. C. (1976). A simple model for estimating the transmittance of direct solar radiation through clear atmospheres. *Solar Energy*, *18*(2), 129–134.

Jablonski, A. (2021). Signal Processing Algorithms BT - Condition Monitoring Algorithms in MATLAB®. In A. Jablonski (Ed.) (pp. 49–194). Cham: Springer International Publishing. https://doi.org/10.1007/978-3-030-62749-2_4

Jestin, Y. (2012). 1.26 - Down-Shifting of the Incident Light for Photovoltaic Applications. In A. B. T.-C. R. E. Sayigh (Ed.) (pp. 563–585). Oxford: Elsevier. https://doi.org/https://doi.org/10.1016/B978-0-08-087872-0.00131-1

Kalogirou, S. (2009). *Solar Energy Engineering: Processes and Systems*. *Solar Energy Engineering* (First). Elsevier. https://doi.org/10.1016/B978-0-12-374501-9.00014-5

Kalogirou, S. A. (1996). Design and construction of a one-axis sun-tracking system. *Solar Energy*, *57*(6), 465–469. https://doi.org/10.1016/S0038-092X(96)00135-1

Kim, Y., Han, G., & Seo, T. (2008). An evaluation on thermal performance of CPC solar collector. *International Communications in Heat and Mass Transfer*, *35*(4), 446–457.

Kivrak, S., Gunduzalp, M., & Dincer, F. (2012). Theoretical and experimental performance investigation of a two-axis solar tracker under the climatic condition of Denizli, Turkey. *Przegląd Elektrotechniczny*, *88*(2), 332–336.

Klassen, A., Rübner, M., Ilg, J., Rupitsch, S. J., Lerch, R., Singer, R. F., & Körner, C. (2012). Influence of the fabrication process on the functionality of piezoceramic patch transducers embedded in aluminum die castings. *Smart Materials and Structures*, *21*(11). https://doi.org/10.1088/0964-

1726/21/11/115014

Koyuncu, B., & Balasubramanian, K. (1991). A microprocessor controlled automatic sun tracker. *IEEE Transactions on Consumer Electronics*, *37*(4), 913–917. https://doi.org/10.1109/30.106958

Lee, C. D., Huang, H. C., & Yeh, H. Y. (2013). The development of sun-tracking system using image processing. *Sensors (Switzerland)*, *13*(5), 5448–5459. https://doi.org/10.3390/s130505448

Lee, H. G., Kim, S. S., Kim, S. J., Park, S.-J., Yun, C., & Im, G. (2015). Development of a hybrid solar tracking device using a GPS and a photo-sensor capable of operating at low solar radiation intensity. *Journal of the Korean Physical Society*, *67*(6), 980–985. https://doi.org/10.3938/jkps.67.980

Liang, K., Zhao, M., Lin, J., Jiao, J., & Ding, C. (2020). An encoder information-based anomaly detection method for planetary gearbox diagnosis. *Measurement Science and Technology*, *31*(4), 45015. https://doi.org/10.1088/1361-6501/ab5b65

Lotti Zadeh. (1965). Fuzzy sets. *Information and Control*, *8*(3), 338–353.

Lucklum, F., & Dumstorff, G. (2017). 3D printed pressure sensor with screen-printed resistive read-out. *Proceedings of IEEE Sensors*, 5–7. https://doi.org/10.1109/ICSENS.2016.7808633

Luque-Heredia, I., Gordillo, F., & Rodriguez, F. (2004). A PI based hybrid sun tracking algorithm for photovoltaic concentration. *Proceedings of the IEEE 19th European Photovoltaic Energy Conversion*, 7–14.

Lynch, W. A., & Salameh, Z. M. (1990). Simple electro-optically controlled dual-axis sun tracker. *Solar Energy*, *45*(2), 65–69.

https://doi.org/https://doi.org/10.1016/0038-092X(90)90029-C

Maatallah, T., El Alimi, S., & Nassrallah, S. Ben. (2011). Performance modeling and investigation of fixed, single and dual-axis tracking photovoltaic panel in Monastir city, Tunisia. *Renewable and Sustainable Energy Reviews*, *15*(8), 4053–4066. https://doi.org/https://doi.org/10.1016/j.rser.2011.07.037

Mamdani, E. H. (1974). Application of fuzzy algorithms for control of simple dynamic plant. In *Proceedings of the institution of electrical engineers* (Vol. 121, pp. 1585–1588). IET.

Matlab. (2020). *Tutorial on TSA Method*.

Mavromatakis, F., & Franghiadakis, Y. (2008). A highly efficient novel azimuthal heliotrope. *Solar Energy*, *82*(4), 336–342. https://doi.org/https://doi.org/10.1016/j.solener.2007.09.001

Messenger, R. A., & Abtahi, A. (2017). *Photovoltaic systems engineering*. CRC press.

Miner, G. L., Ham, J. M., & Kluitenberg, G. J. (2017). A heat-pulse method for measuring sap flow in corn and sunflower using 3D-printed sensor bodies and low-cost electronics. *Agricultural and Forest Meteorology*, *246*(June), 86–97. https://doi.org/10.1016/j.agrformet.2017.06.012

N. H. Helwa, A. B. G. Bahgat, A. M. (2000). Maximum Collectable Solar Energy by Different Solar Tracking Systems. *Energy Sources*, *22*(1), 23–34. https://doi.org/10.1080/00908310050014180

NASA. (n.d.). *ASDC Earth Data*. Retrieved August 1, 2021, from eosweb.larc.nasa.gov

Nsengiyumva, W., Chen, S. G., Hu, L., & Chen, X. (2018). Recent advancements and challenges in Solar Tracking Systems (STS): A review. *Renewable and Sustainable Energy Reviews*, *81*(April 2017), 250–279. https://doi.org/10.1016/j.rser.2017.06.085

Owusu, P. A., & Asumadu-Sarkodie, S. (2016). A review of renewable energy sources, sustainability issues and climate change mitigation. *Cogent Engineering*, *3*(1), 1167990.

Passino, K. M., Yurkovich, S., & Reinfrank, M. (1998). *Fuzzy control* (Vol. 42). Citeseer.

Pehlivan, İ. (2001). *Bulanık mantık kontrolörler ile klasik PID kontrolörlerin karşılaştırılması ve bir bulanık mantık kontrolör tasarımı*. Master Thesis, Sakarya Üniversitesi, Sakarya .

Pita, L. C., San Roman, S. E., Giron-Sierra, J. M., Barriga, J. R., de Vicente, P. D., & Jerez, M. A. (2014). Getting more performance from INTA NanoSat-1B truncated pyramid sun sensors. *IEEE Sensors Journal*, *14*(6), 1867–1877.

Poulek, V., & Libra, M. (2000). A very simple solar tracker for space and terrestrial applications. *Solar Energy Materials and Solar Cells*, *60*(2), 99–103. https://doi.org/https://doi.org/10.1016/S0927-0248(99)00071-9

Qiu, L., Ono, L. K., & Qi, Y. (2018). Advances and challenges to the commercialization of organic–inorganic halide perovskite solar cell technology. *Materials Today Energy*, *7*, 169–189. https://doi.org/https://doi.org/10.1016/j.mtener.2017.09.008

Reda, I., & Andreas, A. (2004). Solar position algorithm for solar radiation applications. *Solar Energy*, *76*(5), 577–589. https://doi.org/https://doi.org/10.1016/j.solener.2003.12.003

Research, L. (2010). Oslo Optics Software.

Roslan, N., Ya'acob, M. E., Radzi, M. A. M., Hashimoto, Y., Jamaludin, D., & Chen, G. (2018). Dye Sensitized Solar Cell (DSSC) greenhouse shading: New insights for solar radiation manipulation. *Renewable and Sustainable Energy Reviews*, *92*, 171–186.

Rubio, F. R., Ortega, M. G., Gordillo, F., & López-Martínez, M. (2007). Application of new control strategy for sun tracking. *Energy Conversion and Management*, *48*(7), 2174–2184. https://doi.org/10.1016/j.enconman.2006.12.020

Saari, M., Xia, B., Cox, B., Krueger, P. S., Cohen, A. L., & Richer, E. (2016). Fabrication and Analysis of a Composite 3D Printed Capacitive Force Sensor. *3D Printing and Additive Manufacturing*, *3*(3), 137–141. https://doi.org/10.1089/3dp.2016.0021

Saavedra, A. S. (1963). *Diseño de un servomecanismo seguidor solar para un instrumento registrador de la irradiación solar directa.* Master Thesis, Universidad Técnica Federico Santa Maria, Valparaiso, Chile.

Samanta, A., Dutta, A., & Neogi, S. (2012). A simple and efficient sun tracking mechanism using programmable logic controller. *Applied Solar Energy*, *48*(3), 218–227. https://doi.org/10.3103/S0003701X12030140

Sen, Z. (2008). *Solar energy fundamentals and modeling techniques: atmosphere, environment, climate change and renewable energy*. Springer Science & Business Media.

Sidek, M. H. M., Hasan, W. Z. W., Kadir, M. Z. A. A., Shafie, S., Radzi, M. A. M., Ahmad, S. A., & Marhaban, M. H. (2014). GPS based portable dual-axis solar tracking system using astronomical equation. *Conference Proceeding - 2014*

IEEE International Conference on Power and Energy, PECon 2014, (February 2016), 245–249. https://doi.org/10.1109/PECON.2014.7062450

Sims, R. E. H. (2004). Renewable energy: a response to climate change. *Solar Energy*, *76*(1–3), 9–17.

Skilhagen, S. E. (2010). Osmotic power — a new, renewable energy source. *Desalination and Water Treatment*, *15*(1–3), 271–278. https://doi.org/10.5004/dwt.2010.1759

Smith, C. L. (2012). The energy challenge. *Applied Petrochemical Research*, *2*(1), 3–6.

Suarez, J. A., & Luengo, C. A. (2003). Coffee husk briquettes: a new renewable energy source. *Energy Sources*, *25*(10), 961–967.

Takagi, T., & Sugeno, M. (1985). Fuzzy identification of systems and its applications to modeling and control. *IEEE Transactions on Systems, Man, and Cybernetics*, (1), 116–132.

Thomas, P. (2017). Computer Based Solar Position Tracking Using Astronomical Algorithms Equations Obtain Position of The Sun, (12), 33–36.

Tina, G. M., Arcidiacono, F., & Gagliano, A. (2013). Intelligent sun-tracking system based on multiple photodiode sensors for maximisation of photovoltaic energy production. *Mathematics and Computers in Simulation*, *91*, 16–28.

Tremante, P., Yen, K., & Brea, E. (2019). Tuning of the membership functions of a fuzzy control system using pattern search optimization method. *Journal of Intelligent & Fuzzy Systems*, *37*(3), 3763–3776.

Vaezi, M., Seitz, H., & Yang, S. (2013). A review on 3D micro-additive manufacturing technologies. *International Journal of Advanced Manufacturing*

Technology, *67*(5–8), 1721–1754. https://doi.org/10.1007/s00170-012-4605-2

Vincent, O. R., & Folorunso, O. (2009). A descriptive algorithm for sobel image edge detection. In *Proceedings of Informing Science & IT Education Conference (InSITE)* (Vol. 40, pp. 97–107).

Vishay Semiconductors. (2004). Temt6000. *Datasheet*, *1.2*(81579), 1–6.

Wei, M.-S., Xing, F., Li, B., & You, Z. (2011). Investigation of Digital Sun Sensor Technology with an N-Shaped Slit Mask. *Sensors* . https://doi.org/10.3390/s111009764

Yang, C.-K., Cheng, T.-C., Cheng, C.-H., Wang, C.-C., & Lee, C.-C. (2017). Open-loop altitude-azimuth concentrated solar tracking system for solar-thermal applications. *Solar Energy*, *147*, 52–60. https://doi.org/https://doi.org/10.1016/j.solener.2017.03.014

Zhang, L., & Hu, N. (2019). Time Domain Synchronous Moving Average and its Application to Gear Fault Detection. *IEEE Access*, *7*, 93035–93048. https://doi.org/10.1109/ACCESS.2019.2927762

Zhou, Z., Chen, J., Hu, Z., Nie, D., & Wen, C. (2021). Design of Solar Dish/Stirling Rotation Control System with Dual Axis Solar Tracker. In *2021 40th Chinese Control Conference (CCC)* (pp. 5794–5799). https://doi.org/10.23919/CCC52363.2021.9549355

APPENDICES

APPENDIX 1: Nomenclature

E	Energy
h	Plank Constant
v	Frequency
c	Speed of Light
λ	Wavelength
Θ_z	Zenith Angle
δ	Declination Angle
n	Day of year
ω	Hour Angle
α_s	Solar Elevation
φ	Latitude
γ_s	Azimuth Angle
I_{ON}	Solar Constant Irradiation (W/m^2)
I_{cbhz}	Direct Solar Irradiation (W/m^2)
I_{cdhz}	Diffuse Solar Irradiation (W/m^2)
I_{cthz}	Total Solar Irradiation (W/m^2)
τ_b	Direct Solar Beam Permeability
τ_d	Diffuse Solar Beam Permeability
β	Inclination Angle

APPENDIX 2: Abbreviations

GPS	Global Positioning System
LDR	Light Dependent Resistor
PLC	Programmable Logic Controller
PI	Proportional Integral
MSE	Mean Square Error
CCD	Charge-coupled Detector
MEMS	Micro-ElectroMechanical System
AM	Air Mass
RTC	Real Time Clock
MTF	Modulation Transfer Function
CSP	Concentrated Solar Power
CAN	Controller Area Network
AM	Additive Manufacturing
FDM	Fused Deposition Modeling
PLA	Polylactic Acid
ADC	Analog Digital Converter
TSA	Time- Synchronous Average
MAD	Mean Absolute Deviation
RMSE	Root Mean Square Error
MAPE	Mean Absolute Percentage Error

APPENDIX 3: Direct Solar Beam Permeability

$\tau_b = a_0 + a_1 e^{-k/\cos\Theta_z}$

These constants are for locations with a 23 km field of view and an altitude of less than 2.5 km.:

$a_0 = r_0\, a_0^*$ $a_1 = r_1\, a_1^*$ $k = r_k\, k^*$

$a_0^* = 0.4237 - 0.00821(6 - A)^2$

$a_1^* = 0.5055 + 0.00595\,(6.5 - A)^2$

$k^* = 0.2711 + 0.01858\,(2.5 - A)^2$ (A=Altitude)

Climate Type	**R_0**	**r_1**	**r_k**
Tropical	0.95	0.98	1.02
Mid Latitude, summer	0.97	0.99	1.02
Subarctic, summer	0.99	0.99	1.01
Mid Latitude, winter	1.03	1.01	1.00

APPENDIX 4: PCB Schematics and Layout

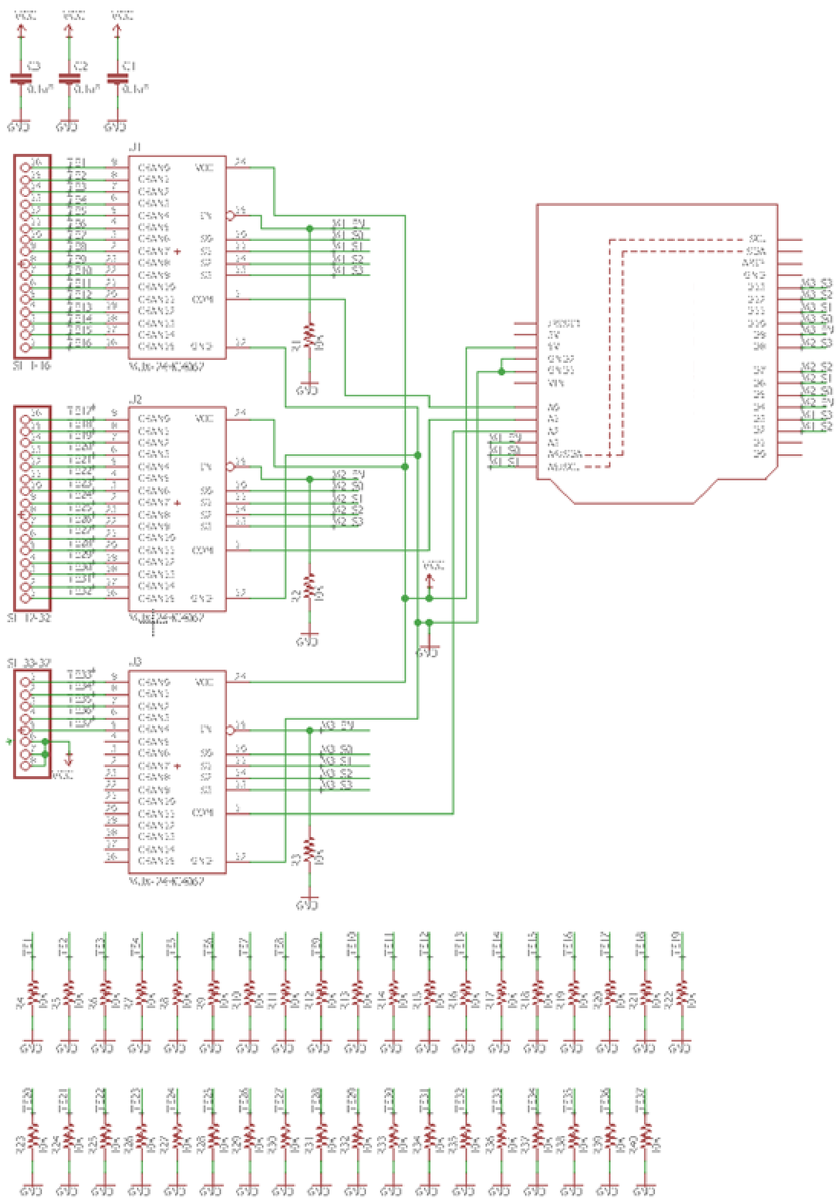

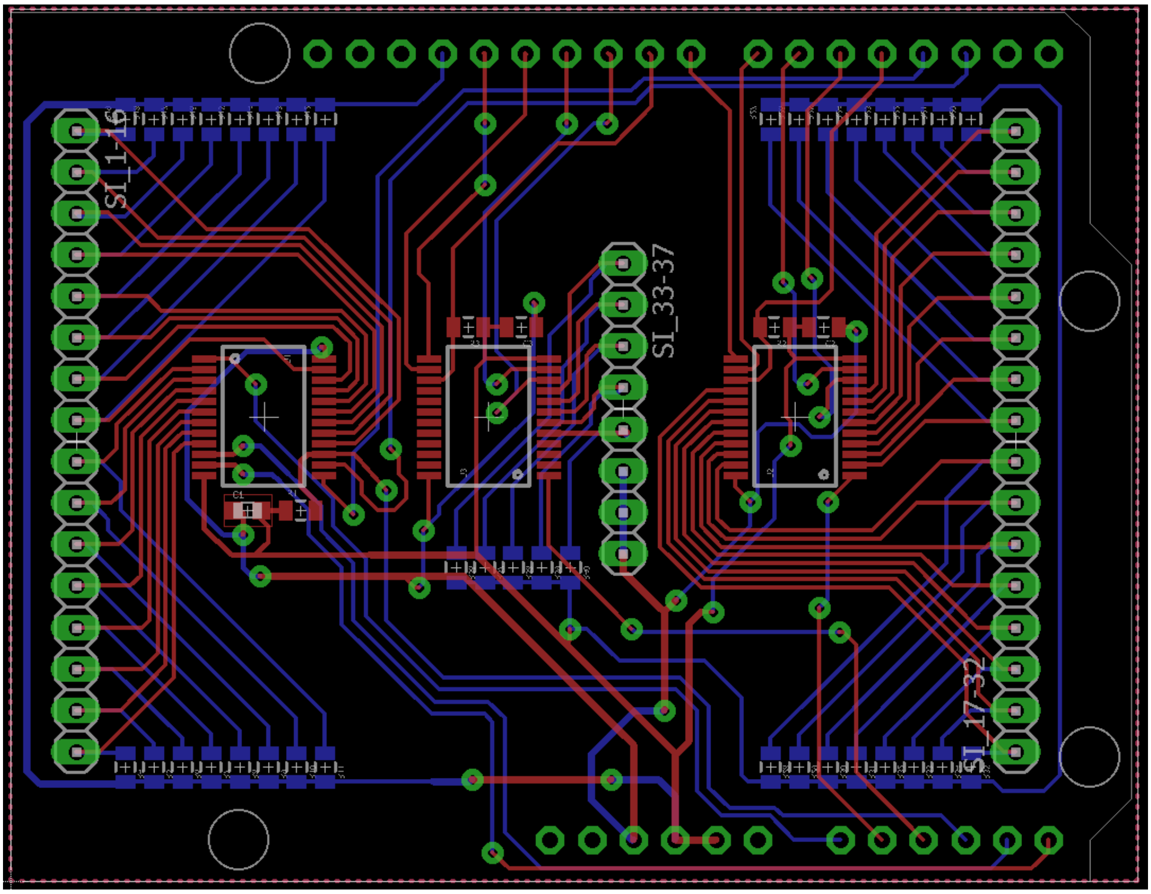
SI_1-16
SI_33-37
SI_17-32
C1

APPENDIX 5: Sensor Measurement Codes

```
const int SIG = A0;// SIG pin
const int EN = A3;// Enable pin
const int controlPin[4] = {18, 19, 2, 3};

const int SIG2 = A1;// SIG pin
const int EN2 = 4;// Enable pin
const int controlPin2[4] = {5, 6, 7, 8};

const int SIG3 = A2;// SIG pin
const int EN3 = 9;// Enable pin
const int controlPin3[4] = {10, 11, 12, 13};

int loopDelay =1;// delay in loop  /15 - 0.1 -0.4 - idi
int sum;
int checksum;
byte M_count=1;
byte NumberofValues=0;
const int muxTable[16][4] = {
    {0,  0,  0,  0}, // 0
    {1,  0,  0,  0}, // 1
    {0,  1,  0,  0}, // 2
    {1,  1,  0,  0}, // 3
    {0,  0,  1,  0}, // 4
    {1,  0,  1,  0}, // 5
    {0,  1,  1,  0}, // 6
    {1,  1,  1,  0}, // 7
    {0,  0,  0,  1}, // 8
    {1,  0,  0,  1}, // 9
    {0,  1,  0,  1}, // 10
    {1,  1,  0,  1}, // 11
    {0,  0,  1,  1}, // 12
    {1,  0,  1,  1}, // 13
    {0,  1,  1,  1}, // 14
    {1,  1,  1,  1}  // 15
};

int ReceivedValues[37];

void setup() {

  for(int i=0; i<4; i++)
  {
    pinMode(controlPin[i], OUTPUT);
    digitalWrite(controlPin[i], HIGH);
```

```
    pinMode(controlPin2[i], OUTPUT);
    digitalWrite(controlPin2[i], HIGH);

    pinMode(controlPin3[i], OUTPUT);
    digitalWrite(controlPin3[i], HIGH);
  }
    pinMode(SIG, OUTPUT);
    digitalWrite(SIG, LOW);

    pinMode(EN, OUTPUT);
    digitalWrite(EN, LOW);
    pinMode(SIG2, OUTPUT);
    digitalWrite(SIG2, LOW);

    pinMode(EN2, OUTPUT);
    digitalWrite(EN2, LOW);

    pinMode(SIG3, OUTPUT);
    digitalWrite(SIG3, LOW);

    pinMode(EN3, OUTPUT);
    digitalWrite(EN3, LOW);

    Serial.begin(2000000);
}
int channelControl(int relayChannel, int M_count)
{
   if (M_count==1) {
    digitalWrite(controlPin[0], muxTable[relayChannel][0]);
    digitalWrite(controlPin[1], muxTable[relayChannel][1]);
    digitalWrite(controlPin[2], muxTable[relayChannel][2]);
    digitalWrite(controlPin[3], muxTable[relayChannel][3]);
//    delay(1);
//    Serial.print(relayChannel);
//    Serial.print (": ");
    pinMode(SIG, INPUT);
//    Serial.println(analogRead(SIG));
//    Value=analogRead(SIG);
    return analogRead(SIG);
    //pinMode(SIG, OUTPUT);

    }
  else if (M_count==2) {
    digitalWrite(controlPin2[0], muxTable[relayChannel][0]);
    digitalWrite(controlPin2[1], muxTable[relayChannel][1]);
    digitalWrite(controlPin2[2], muxTable[relayChannel][2]);
    digitalWrite(controlPin2[3], muxTable[relayChannel][3]);
      //Serial.println ("---2.tur---");
```

```
 pinMode(SIG2, INPUT);
 return analogRead(SIG2);

 }
 else if (M_count==3 && relayChannel<=4) {

   digitalWrite(controlPin3[0], muxTable[relayChannel][0]);
   digitalWrite(controlPin3[1], muxTable[relayChannel][1]);
   digitalWrite(controlPin3[2], muxTable[relayChannel][2]);
   digitalWrite(controlPin3[3], muxTable[relayChannel][3]);
     //Serial.print ("---3.tur---");

   pinMode(SIG3, INPUT);

   return analogRead(SIG3);
}

}//channelControl end

void Send_Data (int ReceivedValues[], int n) {
 sum=0;
 Serial.print(":");Serial.print(n,HEX);
 for (int i=0;i<n;i++)
   {
     if(ReceivedValues[i]<16)
{Serial.print(0,HEX);Serial.print(0,HEX);Serial.print(ReceivedValues[i],HEX);sum
=sum+ReceivedValues[i];}

     if(ReceivedValues[i]>=16 && ReceivedValues[i]<256)
{Serial.print(0,HEX);Serial.print(ReceivedValues[i],HEX);sum=sum+ReceivedValu
es[i];}

     if(ReceivedValues[i]>=256)
{Serial.print(ReceivedValues[i],HEX);sum=sum+ReceivedValues[i];}

   }
    checksum=0xFF-(sum & 0xFF);
     if(checksum<16)
{Serial.print(0,HEX);Serial.print(checksum,HEX);Serial.println();}
     else {Serial.print(checksum,HEX);Serial.println();}
//   Serial.println();
}

int Count_Values (int ReceivedValues[], int n) {
 for (int i=0;i<n;i++) {
  if (ReceivedValues[i] >= 0) { NumberofValues=37;}
 return NumberofValues;
}
```

```
}

void loop() {

  for(int i=0; i<16; i++)
  {
  if (M_count==1) { ReceivedValues[i]=channelControl(i,M_count);
//  Serial.print(ReceivedValues[i])+Serial.print(" ");
}

  if (M_count==2) { ReceivedValues[i+16]=channelControl(i,M_count);
//  Serial.print(ReceivedValues[i+16])+Serial.print(" ");
  };

  if (M_count==3 && i<=4) {ReceivedValues[i+32]=channelControl(i,M_count);
//  Serial.print(ReceivedValues[i+32])+Serial.print(" ");
  }

//delay(loopDelay);// wait for loopDelay ms
delayMicroseconds(loopDelay);
  }

  M_count++;
   if (M_count==4)
  {
     delayMicroseconds(1);
     M_count=1;
      NumberofValues=Count_Values(ReceivedValues,37);
      Send_Data(ReceivedValues,NumberofValues);
  }
}
```